

Alma Mater Studiorum Università di Bologna  
Archivio istituzionale della ricerca

Linking Holocene vegetation dynamics, palaeoclimate variability and depositional patterns in coastal successions: Insights from the Po Delta plain of northern Italy

This is the final peer-reviewed author's accepted manuscript (postprint) of the following publication:

*Published Version:*

Linking Holocene vegetation dynamics, palaeoclimate variability and depositional patterns in coastal successions: Insights from the Po Delta plain of northern Italy / Cacciari M.; Amorosi A.; Marchesini M.; Kaniewski D.; Bruno L.; Campo B.; Rossi V.. - In: PALAEOGEOGRAPHY PALAEOCLIMATOLOGY PALAEOECOLOGY. - ISSN 0031-0182. - ELETTRONICO. - 538:(2020), pp. 109468.1-109468.16. [10.1016/j.palaeo.2019.109468]

*Availability:*

This version is available at: <https://hdl.handle.net/11585/728045> since: 2020-02-25

*Published:*

DOI: <http://doi.org/10.1016/j.palaeo.2019.109468>

*Terms of use:*

Some rights reserved. The terms and conditions for the reuse of this version of the manuscript are specified in the publishing policy. For all terms of use and more information see the publisher's website.

This item was downloaded from IRIS Università di Bologna (<https://cris.unibo.it/>).  
When citing, please refer to the published version.

(Article begins on next page)

This is the final peer-reviewed accepted manuscript of:

**Cacciari, M., Amorosi, A., Marchesini, M., Kaniewski, D., Bruno, L., Campo, B., & Rossi, V. (2020). Linking holocene vegetation dynamics, palaeoclimate variability and depositional patterns in coastal successions: Insights from the po delta plain of northern italy. *Palaeogeography, Palaeoclimatology, Palaeoecology*, 538**

The final published version is available online at  
<https://dx.doi.org/10.1016/j.palaeo.2019.109468>


Rights / License:

The terms and conditions for the reuse of this version of the manuscript are specified in the publishing policy. For all terms of use and more information see the publisher's website.

*This item was downloaded from IRIS Università di Bologna (<https://cris.unibo.it/>)*

***When citing, please refer to the published version.***

# Linking Holocene vegetation dynamics, palaeoclimate variability and depositional patterns in coastal successions: Insights from the Po Delta plain of northern Italy

 The corrections made in this section will be reviewed and approved by journal production editor.

Marco **Cacciari**<sup>a,\*</sup> [marco.cacciari3@unibo.it](mailto:marco.cacciari3@unibo.it), Alessandro **Amorosi**<sup>a</sup>, Marco **Marchesini**<sup>b</sup>, David **Kaniewski**<sup>c</sup>, Luigi **Bruno**<sup>d</sup>, Bruno **Campo**<sup>a</sup>, Veronica **Rossi**<sup>a</sup>

<sup>a</sup>Dipartimento di Scienze Biologiche, Geologiche e Ambientali, University of Bologna, via Zamboni 67, 40127 Bologna, Italy

<sup>b</sup>Department of Human and Social Sciences, University of Ferrara, via Ercole I d'Este 32, 44121 Ferrara, Italy

<sup>c</sup>Université Paul Sabatier-Toulouse 3, EcoLab (Laboratoire d'Ecologie Fonctionnelle et Environnement), 118 Route de Narbonne, 31062, Toulouse, cedex 9, France

<sup>d</sup>Department of Chemical and Geological Sciences, University of Modena, via Campi 103, 44125 Modena, Italy

\*Corresponding author.

---

## Abstract

Mediterranean deltaic-coastal plains represent relatively underexplored depositional archives that record the Holocene response of vegetation and depositional systems to high-frequency climate changes. In this study, we examine a 25 m-thick succession of Holocene age (core EM2) recovered in the innermost portion of the Po delta plain of northern Italy, applying an integrated palynostratigraphic approach. The existence of a paludal, freshwater setting inland of the line of maximum marine transgression favoured a low degree of pollen transportation. Application of cluster analysis to this palynological record leads to the identification of pollen-derived biomes and seven (auto)ecological groups of taxa that discriminate environmental signal (depositional facies) and regional climate conditions within a well-dated coastal record. Percentage variations of

hygrophytes, aquatics and pasture-meadow herbs reveal local environmental dynamics, enabling the detailed facies ~~characterization~~characterisation of the cored succession, especially in terms of water table conditions. Framed into a chronologically constrained, high-resolution facies context, the proportion of montane taxa (climate degradation indicator) relative to Mediterranean taxa and *Quercus* + other deciduous trees (climate optimum indicators) highlight a vegetation-climate variability in the plain that fits with Bond events, especially for the early-mid Holocene (i.e., Preboreal and Boreal Oscillation, 8.2 ka event), supporting a strong Mediterranean–North Atlantic climate connection. For the first time, pollen from a continental succession of the Adriatic area clearly depicts the effects of the 8.2 ka cooling event on vegetation patterns (progressive degradation in high altitude communities) and depositional dynamics (increased fluvial activity), assessing the major role played by climate changes in shaping coastal landscapes in addition to glacio-eustatic variations.

---

**Keywords:** Palynology; Adriatic area; 8.2 ka event; Palaeoenvironment; Freshwater swamp

## 1.1 Introduction

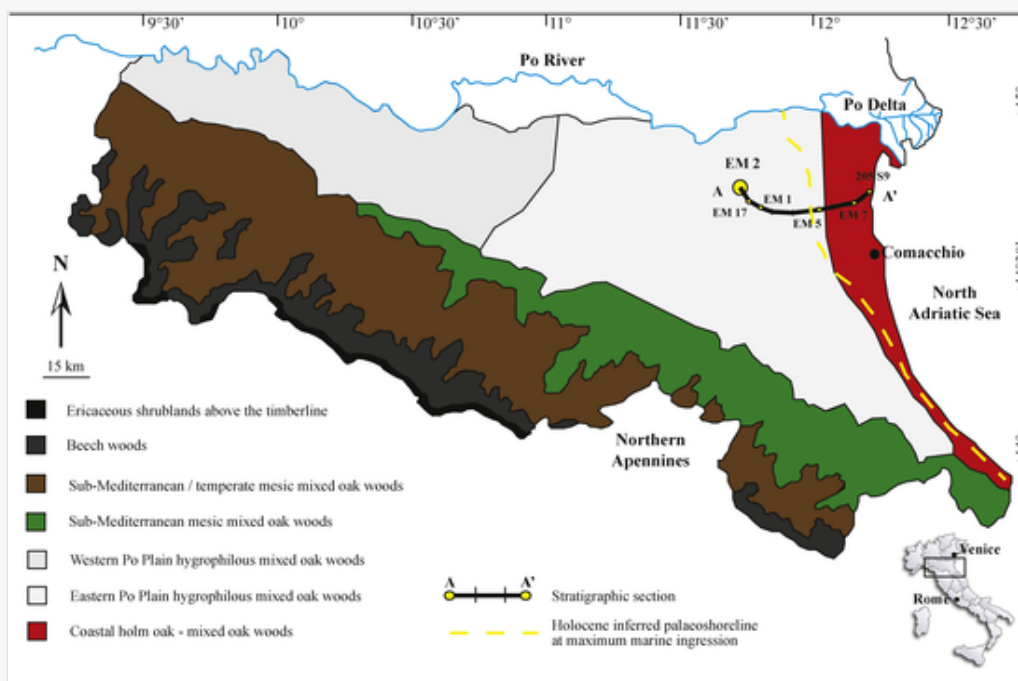
The diversity of palaeoclimate proxies (e.g., microfossils, molluscs, stable isotopes), the abundance of effective dating techniques (e.g., radiocarbon and other radiometric dating, amino acid racemization), and the temporal proximity to the Present have made the climate variability of Marine Isotope Stage-MIS 1 (ca. last 15 kyr) a focus of research in recent decades (e.g., [Sangiorgi et al., 2003](#); [Magny et al., 2007](#); [Giraudi et al., 2011](#); [Scarponi et al., 2017](#); [Bini et al., 2019](#); [Di Rita and Magri, 2019](#)). Since the pioneer works of Bond and colleagues on the North Atlantic deep-sea successions (the well-known “Bond events”; Bond et al., 1993, [Bond et al., 1997](#)) and the review by Mayewski and colleagues on the Holocene record (Rapid Climate Changes-RCC; [Mayewski et al., 2004](#)), the millennial to sub-millennial climate oscillations of MIS 1 and related environmental-depositional responses have attracted increasing interest ([Benito et al., 2015a, 2015b](#); [Di Rita et al., 2015](#); [Sarti et al., 2015](#); [Styllas and Ghilardi, 2017](#); [Roberts et al., 2019](#) among others). Special emphasis has been placed on the origin, geographical distribution, amplitude and characterisation of three major events during this period (Younger Dryas, 8.2 ka and 4.2 ka), corresponding to the chronostratigraphic limits of the Holocene subseries (Lower, Middle and Upper Holocene; [Walker et al., 2012](#); International Commission on Stratigraphy, 2018). However, several other short-term events have been identified across the globe (i.e., Preboreal and Boreal Oscillations; Little Ice Age among others) and highlight a high-frequency climate variability for different regions and latitudes (e.g., [Magny et al., 2013](#); [Vanni re et al., 2011](#); [Feurdean et al., 2007](#)).

In such a complex scenario, pollen is considered one of the most powerful palaeoclimate proxies because of its high degree of preservation (Faegri et al., 1989; Moore et al., 1991) and its capacity to furnish detailed (vegetation-derived) reconstructions. For the Mediterranean area, millennial-scale palaeoclimate patterns have been revealed mainly by a variety of lacustrine and marine pollen records (e.g., [Peyron et al., 2011, 2013](#); [Magny et al., 2012](#)). However, pollen records from the Adriatic region very seldom encompass the whole MIS 1 (e.g., [Di Rita and Magri, 2009](#); [Magny et al., 2009](#); [Mercuri et al., 2012](#); [Ravazzi et al., 2013](#); [Cremaschi et](#)

al., 2016; Pini et al., 2016; Badino et al., 2018) because of either local environmental conditions (e.g., lake formation and damming) or anthropic presence (e.g., archaeological sites), with the unique exception of a south Adriatic marine core (Combourieu-Nebout et al., 2013). Despite an abundance of relatively continuous, tens of meters thick paludal successions (Amorosi et al., 2017a), prone to preserve palynomorphs (Cacciari et al., 2018), and thorough understanding of present-day vegetation landscapes (Tomaselli, 1970; Pignatti, 1979, 1998; Ferrari, 1980, 1997), the Holocene coastal succession of the modern Po delta plain (N Italy; Fig. 1) represents a relatively underexplored depositional archive to probe vegetation-palaeoclimate reconstructions. In this area, the availability of robust, high-resolution chronological and sequence-stratigraphic frameworks (i.e., Amorosi et al., 2016, 2017a, 2017b; Bruno et al., 2017; Campo et al., 2017) makes these deposits an ideal archive to investigate climate-related palaeoenvironmental variations. The main purpose of this work is to document the possibility of filtering the local (facies) vegetation signal from the regional (climate) record, relying upon a continuous Holocene pollen record from an unconventional (i.e., non-lacustrine and non-marine) succession of the Po delta plain (core EM2; Fig. 1), whose general palynological features (i.e., relative percentages of groups of taxa) have been published in Cacciari et al. (2018). More specifically, through an integrated, high-resolution stratigraphic-palynological approach supported by the application of statistical analyses, we aim to: *i*) obtain new data on vegetation-climate dynamics of the Adriatic area, verifying the timing and effects of North Atlantic climate oscillations (i.e., Bond's events), and *ii*) furnish insights into the effects of Holocene climate variability on the depositional dynamics of deltaic-coastal plain systems.

alt-text: Fig. 1

Figure 1. Fig. 1



Location map showing the vegetation zonation of the Emilia-Romagna region of northern Italy (partly redrawn after Ferrari, 1997 and Regione Emilia-Romagna, 1996) and location of core EM2. The inferred position of the Holocene maximum marine ingress is also shown (slightly modified from Correggiari et al., 2005 and Bruno et al., 2017).

## 2.2 Study area

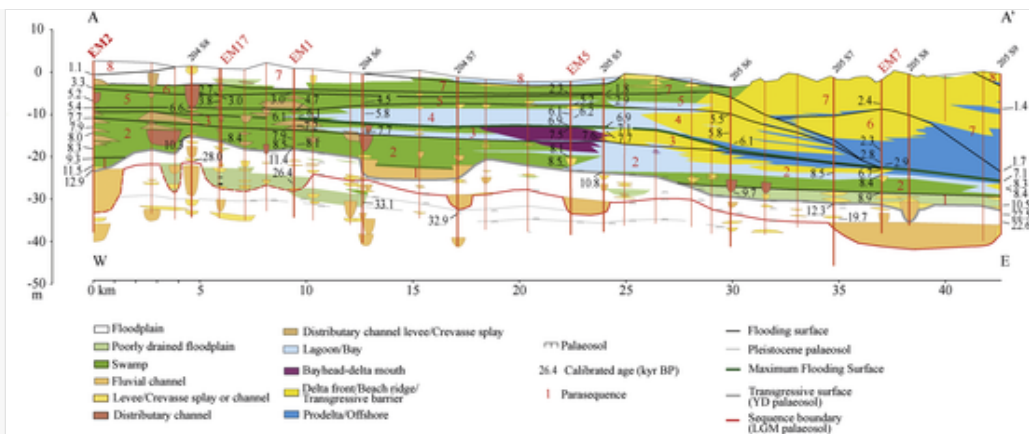
### 2.1.2.1 Geological setting and Quaternary stratigraphic framework

The Po delta plain is a wide flat area (ca. 3000 km<sup>2</sup>) with around 1550 km<sup>2</sup> lying below mean sea level (Bondesan et al., 1999; Correggiari et al., 2005). It includes the modern Po Delta, a mixed, river- and wave-influenced system formed during the last 2 kyr (Amorosi et al., 2008; Rossi and Vaiani, 2008; Maselli and Trincardi, 2013) and the southern coastal plain occupied by palaeodelta lobes that were active between ca. 7.0–2.0 kyr BP (Fig. 1; Stefani and Vincenzi, 2005; Amorosi et al., 2019). At the basin scale, the Po delta plain constitutes the eastern portion of the broader Po Plain, which is the surficial expression of the peri-sutural Po Basin delimited by the Alps to the north-west and by the N Apennines to the south. To the east, the Po Plain is bounded by the Adriatic Sea, a narrow (ca. 200–800 km) semi-enclosed epicontinental basin elongated in NW-SE direction and sandwiched between the Italian peninsula and the Balkans. As a whole, the Po Plain-Adriatic Sea system is part of the Alpine-Apennine and Dinarides-Hellenides foreland, shaped by the convergence between the European and African plates (Doglioni, 1993; Boccaletti et al., 2011). The infilling succession of the Po Basin records an overall “regressive” trend, from Pliocene deep-marine to Pleistocene-Holocene continental and coastal deposits (Ricci Lucchi et al., 1982; Regione Emilia-Romagna and Eni-Agip, 1998). The Middle Pleistocene-Holocene succession shows the repeated vertical stacking of transgressive-regressive (T-R) depositional cycles, composed of shallow marine, coastal and alluvial deposits accumulated under a predominantly glacio-eustatic control (Milankovitch 100 kyr-cycles; Amorosi et al., 2004; Lobo and Ridente, 2014). In the southern Po coastal plain, palynological analyses further support a climate control on facies architecture, as wedge-shaped coastal bodies identified between ca. 0–30 m and 100–130 m depths record phases of forest expansion associated with the last two interglacials (MIS 1 and MIS 5e, respectively). By contrast, the tens m-thick alluvial succession that separates these two nearshore bodies documents a fall in the arboreal cover and the presence of cold climate indicators, pointing to the MIS 5d-MIS 2 glacial period (Amorosi et al., 2004; Campo et al., 2017).

Recent studies (Amorosi et al., 2017a, 2019; Bruno et al., 2017) have placed the Holocene succession into a high-resolution sequence-stratigraphic framework. Above the Younger Dryas palaeosol, a prominent stratigraphic marker demarcating the transgressive surface (TS), eight parasequences (PSs) were identified (Fig. 2) based on integrated sedimentological, palaeontological (molluscs, benthic foraminifers and ostracods) and radiocarbon data. Early Holocene parasequences (PSs 1–3 in Fig. 2) are organised into a retrogradational pattern reflecting alternating periods of rapid flooding and gradual shoaling into the Po estuary, developed under the predominant control of the postglacial eustatic rise (Bard et al., 1996; Vacchi et al., 2016). By contrast, an aggradational to progradational set of mid-late Holocene parasequences (PSs 4–8 in Fig. 2) mostly controlled by changes in sediment supply, subsidence and autogenic mechanisms records the transition from a wave-dominated to a river-dominated delta system.

alt-text: Fig. 2

Figure 2. Fig. 2



Reference stratigraphic section A-A'<sup>2</sup>, slightly modified from Bruno et al. (2017), showing the Holocene depositional architecture of the Po delta-coastal plain. The transgressive barrier sands belonging to PS 3 mark the Holocene maximum marine ingress in Fig. 1. Key EM cores are highlighted in red; core EM2 is in bold. (For interpretation of the references to colour in this figure legend, the reader is referred to the web version of this article.)

## 2.2.2.2 Present-day vegetation and climate

The study area belongs to the Emilia-Romagna (ER) region (Fig. 1) characterised by a sub-Mediterranean climate, broadly diffused throughout North and Central Italy. The annual precipitation sum is up to 778 mm/yr and decreases during summer, with minimum values in July and August. The mean annual temperature (13.2°C) and thermal excursion (ca. 22°C between July–January means - 23.8°C and 2°C, respectively) suggest a certain degree of continentality (Bologna site; Ubaldi, 2003). The vegetation landscape reflects mixed influences, as the study area is located at the southern margin of the Central European phytogeographic region, adjacent to the Mediterranean area (Tomaselli, 1970; Pignatti, 1979, 1998). The boundary between these two regions is sharp along the Apennine ridge but becomes blurred in the east (Ferrari, 1997), where coastal vegetation occurs as a mix of Central European and euri-Mediterranean taxa. The present vegetation changes not only along a longitudinal gradient (distance from the Adriatic Sea), but also along an altitudinal one (lowlands versus mountains). In order to assess the complex dynamics of vegetation communities, the concept of Potential Natural Vegetation (PNV) by Tüxen (1956) will be hereafter adopted. Though still debated (Carrión and Fernandez, 2009; Chiarucci et al., 2010), PNV has been extensively used by several authors (Blasi et al., 2014; Hengl et al., 2018), who stressed its importance in defining both modern and past vegetation landscapes dynamics. As a whole, three main vegetation belts were identified and can be described as follows (Fig. 1; Ferrari, 1997):

- Ericaceous dwarf shrublands above the timberline* (ca. 1800 m above sea level-a.s.l.): this vegetation belt is discontinuous across ER and absent in its south-eastern portion, due to lower altitudes. The vegetation is similar to the one in the Western and Central Alps (order *Rhododendro – Vaccinietalia* Braun Blanquet 1926) but impoverished in species, as it commonly occurs at the edge of geographic ranges. Since no extensive fir and/or spruce woods occur on the Apennines, the boundary between ericaceous dwarf shrublands and beech woods (Fig. 1) should be considered a real ecotone (Chiarugi, 1958).
- Beech woods*: beech forests occupy a relatively wide and continuous area from NW to SE,



extending from 800-to 1000 m a.s.l. up to the timberline, with the exception of relict fir/spruce woods on the slopes of refugial valleys. This belt includes several species belonging to the *Quercetum*- (*Fraxinus excelsior*, *Tilia platyphyllos*, *Ulmus glabra*) and the montane PNV (*Abies alba* and *Fagus sylvatica*), consistent with the altitude-dependent bioclimatic gradient.

- c) *Mixed mesic oak woods*: as part of the *Quercus – Carpinetum boreoitalicum* (Pignatti, 1953), these forests form a wide vegetation belt extending from 0 to 800 m a.s.l. that represents the Po Plain PNV (Ferrari, 1997; Pignatti, 1998). Lowland communities differ slightly from those living on the hills because of the widespread presence of humid environments. However, intense human activity has almost completely destroyed these mesophilous oak forests (Cattaneo, 1844). Seawards, on stable sand dunes along the coast, a community dominated by *Quercus ilex*, *Fraxinus ornus*, *Asparagus acutifolius* and *Pyracantha coccinea* occurs. A similar vegetation dominated by *Quercus robur*, *Q. ilex* and *Carpinus betulus* characterises the oldest dunes. In particular, the presence of the holm oak marks the shift from a sub-Mediterranean climate inland to a more Mediterranean one along the coast. Both communities belong to the alliance *Ostrya – Carpinion orientalis* (Horvat 1959) and represent the North Adriatic coastal form of mixed oak woodlands, which are still present in the Balkans and on the Adriatic side of the central Apennines.

Focusing on the local vegetation, the study area belongs to the Po Plain Province (ecoregions of Italy sensu Blasi et al., 2014) - Lagoon Subsection spanning about 70 km from the coastal portion of the Venetian Plain, down to the Comacchio lagoons (Fig. 1). It is mainly characterised by cultivated areas (ca. 77%, mostly *Triticum* and *Beta*).

## **3.3** Methods

In order to isolate the signal related to the depositional setting from regional climate conditions, integrated palynological and stratigraphic analyses were undertaken on a long (ca. 25 m) fine-grained succession of Holocene age, recovered in the innermost portion of the Po delta plain (core EM2; Fig. 1). Its location, ca. 25 km landward of the palaeoshoreline at the time of Holocene maximum marine ingression (Fig. 2), strongly limits the influence of marine pollen transportation according to the extreme scarcity (0-3%) of halophytes (i.e., *Artemisia* and *Beta*) already highlighted by Cacciari et al. (2018).

### **3.1.3.1** Core sedimentology and chronology


The 40 m-long core EM2 (44°48'28"N; 11°47'2.5"E; Fig. 1) was recovered at 2.7 m a.s.l. by a continuous perforating system, which guaranteed an undisturbed stratigraphy and a high recovery percentage (>90%). The core was split lengthwise and carefully described in terms of grain size, sedimentary structures, colour, organic-matter content (peat or decomposed organic matter-rich layers), stratigraphic contacts and other materials (i.e., sparse vegetation remains, calcareous and Fe—Mn nodules) in order to identify the main lithofacies. The abundance of organic-rich, peaty deposits supports a high-resolution, radiocarbon-based chronological analysis of the studied succession. Radiocarbon dating on 13 samples was performed at KIGAM laboratory (Daejeon City, Republic of Korea) on wood, plant fragments and peats collected between ca. 3-3



25.50 m core depth (Table 1). The calibration of conventional radiocarbon ages is based on the IntCal13 dataset (Reimer et al., 2013) using OxCal 4.2. (Bronk Ramsey, 2009). All ages are expressed in 2-sigma calibrated years BP. The age-depth model was constructed using a smoothing spline function in PAST (PAlaeontological SStatistic – version 3.10 by Hammer et al., 2001). Differential sediment compaction was not taken into account, thus sedimentation rates were estimated on the basis of radiocarbon ages.

alt-text: Table 1

Table 1: Table 1

 The presentation of Tables and the formatting of text in the online proof do not match the final output, though the data is the same. To preview the actual presentation, view the Proof.

List of radiocarbon dated samples from core EM2.

Sample core depth (m)	Dated material	<sup>14</sup> C conventional age (yr BP)	Calibrated yr BP - 2σ range interval	Calibrated yr BP - 2σ mean value ± error	Reference
3.20	Wood	1180 ± 40	1185 - 980	1085 ± 105	Amorosi et al., 2017a
6.45	plant fragment	3110 ± 80	3485 - 3075	3280 ± 200	Amorosi et al., 2017a
9.45	Wood	4480 ± 30	5240 - 5035	5170 ± 85	This study
11.10	Plant fragment	4680 ± 40	5480 - 5315	5395 ± 80	Amorosi et al., 2017a
13.35	Plant fragment	6840 ± 40	7760 - 7590	7675 ± 85	Amorosi et al., 2017a
14.65	Wood	6630 ± 40	7575 - 7440	7520 ± 35	This study
15.20	Plant fragment	7460 ± 40	8365 - 8190	8280 ± 50	Amorosi et al., 2017a
15.30	Peat	7070 ± 40	7975 - 7825	7900 ± 40	This study
16.60	Wood	7140 ± 40	8025 - 7925	7965 ± 35	This study
20.55	Wood	7470 ± 50	8380 - 8185	8285 ± 95	Amorosi et al., 2017a
22.90	Wood	8320 ± 50	9470 - 9200	9335 ± 135	Amorosi et al., 2017a
24.50	Plant fragment	9990 ± 50	11,650 - 11,260	11,455 ± 195	Amorosi et al., 2017a
25.45	Plant fragment	11,110 ± 50	13,065 - 12,820	12,950 ± 130	Amorosi et al., 2017a

### 3.2.3.2 Palynological analyses

Thirty-five samples from the uppermost 25 metres were collected for palynological analysis. All lithofacies were analysed with a special focus on organic-rich intervals, where abundant palynological assemblages were expected. Samples were prepared and analysed at “*Centro Agricoltura e Ambiente – CAA G. Nicoli*” laboratory (Italy), following a standard extraction technique (Lowe et al., 1996): about 3–9 g of dry sediment were weighed and a *Lycopodium* tablet was added to calculate pollen concentration. Samples were mechanically disrupted in a 10% Na-pyrophosphate solution and filtered through a 0.5 mm sieve and a 5 µm nylon filter. A series of chemical treatments was then applied (10% HCl solution to remove carbonates, acetolysis for excess organics, heavy liquid, 40% HF solution, ethanol suspension for pollen grains enrichment). Following evaporation at 60 °C, microscope slides were prepared with glycerine jelly and paraffin. For each sample, at least 300 pollen grains were counted (where possible) at 400× magnification and recognised using general morphological keys (Faegri et al., 1989; Moore et al., 1991). The CAA laboratory’s collection and published atlases (Reille, 1992, 1995, 1998) were also useful to improve pollen determination. If the conservation degree and orientation (i.e., polar or equatorial view) of grains were favourable, a set of morphological parameters published in literature were used for the determination at species level of alders, oaks, pines and Asteroideae (SOM-S1). If this was not possible, the conservative choice of the higher taxonomical level was made to avoid mis/overinterpretation.

Pollen percentages were calculated on the basis of the total pollen sum. Percentages of Pteridophytes, undeterminable and reworked grains were calculated on the total sum of pollen grains and themselves, a method allowing a correct weighting of their presence (Berglund and Ralska-Jasiewiczowa, 1986).

Species ecological characterisation was based on Tomaselli (1970, 1987), Pignatti (1979, 1982, 2017), Ferrari (1980, 1997), Berglund and Ralska-Jasiewiczowa (1986), Tutin et al. (1993), Accorsi et al. (1999, 2004), Bertoldi (2000), Ubaldi (2003) and Pini et al. (2016).

### 3.2.3.3 Statistical analysis

Following Tarasov et al. (1998) and Kaniewski et al. (2011), we performed statistical analyses to highlight pollen-derived vegetation biomization and support the identification of pollen groups. Spermatophyte and Pteridophyte taxa were calculated in PAST and grouped using Cluster Analysis. Correlation was used as similarity method to explore the temporal proximity of taxa in a facies-heterogeneous stratigraphic succession, while Paired group was used as the root by suggesting the local provenance of all identified taxa. In order to streamline the data and obtain the most informative groups, sixty occasional taxa, recorded in less than three samples with percentages lower than 1%, were excluded. The robustness of this choice was tested by running several analyses using different selections of taxa. The resulting clusters, obtained from a final matrix of 141 taxa, allowed the identification of pollen-derived biomes (PDBs) whose ecological distance is reflected by the branches on the tree diagram (Kaniewski et al., 2011). The use of present-day ER altitudinal-longitudinal vegetation belts (Fig. 1) as a reference for past associations reasonably suggests that PDBs should not be

considered as separate vegetation types but, rather, as groups of plants that can thrive or decrease at the same time close to the sample site (i.e., groups of taxa that were site-dependently found together).

## 4.4 Results

### 4.1.4.1 Pollen data

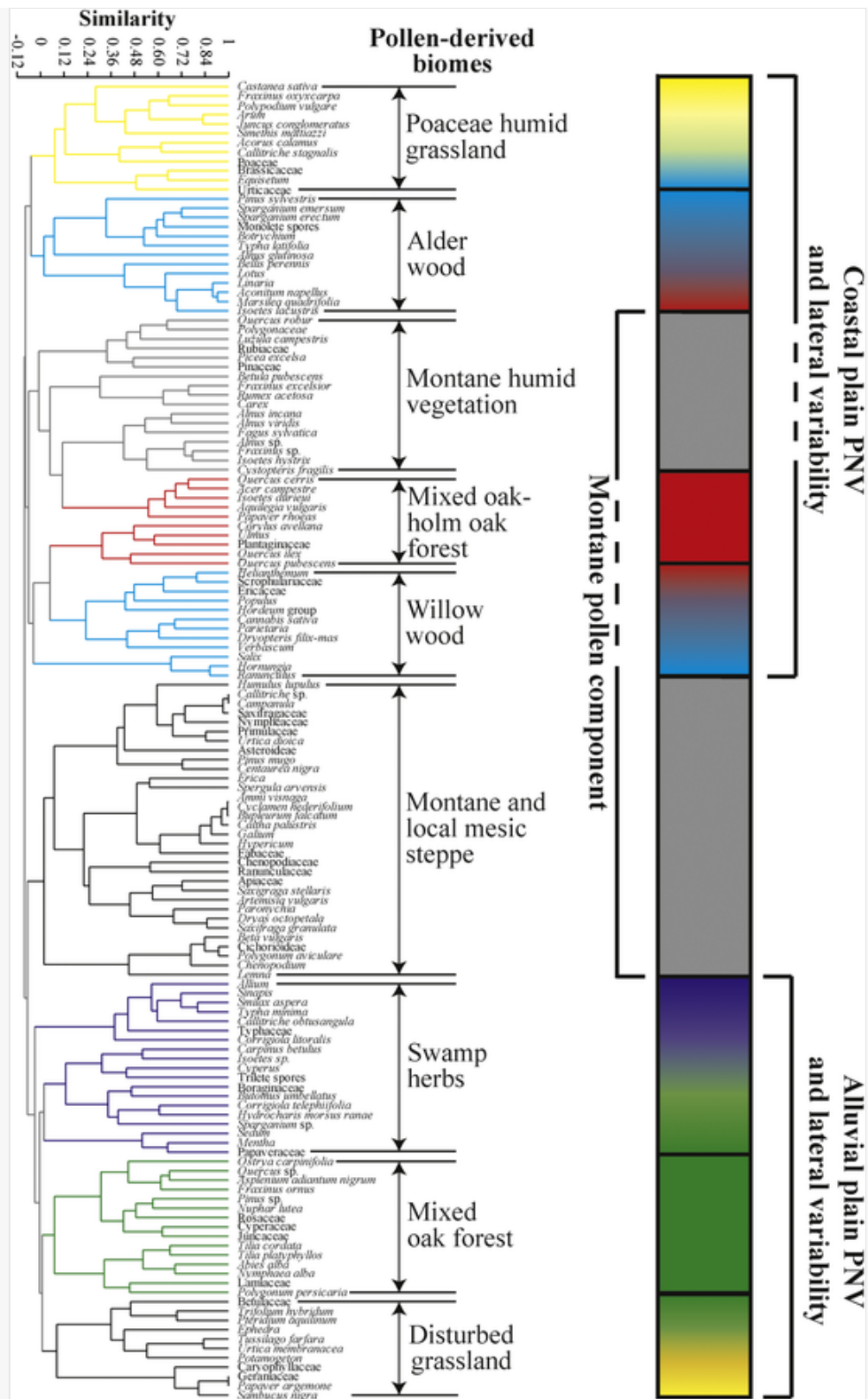
Pollen data from core EM2 reveal a high floristic richness. Specifically, 189 taxa were identified at different taxonomic levels and raw counts are available at Mendeley Data. Consistent with the organic-rich nature of sediments, the state of preservation of pollen grains is good and the number of undeterminable grains varies from 0% to ca. 15%. The relative abundance of secondary grains reworked from older successions is generally lower than 10%.

#### 4.1.1.4.1.1 Pollen-derived biomes

In the cluster analysis of [Fig. 3](#), the tree diagram furnishes a representation of vegetation dynamics in the plain and in the surrounding reliefs. Nine ecologically distinct PDBs were identified ([Fig. 3](#)): Poaceae humid grassland (Phg), Alder wood (Aw), Montane humid vegetation (Mhv), Mixed oak–holm oak forest (Mo-ho), Willow wood (Ww), Montane and local mesic steppe (Mlms), Swamp herbs (Swh), Mixed oak forest (Mof) and Disturbed grassland (Dg). Two PDB super-groups are recognizable at the highest ecological distance and reflect different vegetation communities developed during the climate optimum, i.e., alluvial plain vs. coastal plain PNVs. The former group of taxa mainly includes the mixed oak forest (the PNV of the Po alluvial plain and low hills), while the latter contains Mediterranean taxa (mixed oak-holm oak forest). As a whole, these super-groups are both bracketed by PDBs that reflect the lateral transition to a variety of settings differing in terms of humidity and/or levels of disturbance. Low degrees of humidity are represented by grassland biomes (Dg and Phg in [Fig. 3](#)), while high water table levels are highlighted by wetland biomes typical of swampy environments (Swh, Ww and Aw in [Fig. 3](#)). Two PDBs associated with montane taxa (Mms and Mhv in [Fig. 3](#)) interrupt this trend, suggesting they represent sudden environmental changes not related to local dynamics/lateral facies variability.

alt-text: Fig. 3

[Figure 3](#), [Fig. 3](#)




Tree diagram obtained through cluster analysis performed on selected plant taxa of core EM2 (Correlation similarity method and Paired group root were used). The resulting pollen-derived biomes (PDBs) and interpreted vegetation dynamics in the Po Plain and surrounding reliefs are also shown.

#### 4.1.2.4.1.2 Pollen groups

Seven pollen groups were identified (Table 2) integrating PDBs (Fig. 3), present-day regional vegetation physiognomy (Fig. 1) and specific (auto)ecological features of the identified taxa. Each group is briefly described below.

alt-text: Table 2

Table 2: Table 2

 The presentation of Tables and the formatting of text in the online proof do not match the final output, though the data is the same. To preview the actual presentation, view the Proof.

Pollen groups identified in core EM2 through integration of PDBs, present-day regional vegetation physiognomy and specific (auto)ecological features. Main pollen taxa and the climate and/or environmental significance of each group are reported.

Pollen groups	Main taxa	Proxy in coastal-alluvial contexts
Hyg	Sum of woody taxa ( <i>Alnus glutinosa</i> , <i>Salix</i> ) and herbs (Cyperaceae, various ferns)	Facies indicator (degree of humidity)
Aq	Sum of helophytes ( <i>Isoetes durieui</i> , <i>I. hystrix</i> , <i>Sparganium erectum</i> , <i>Typha</i> ) and hydrophytes (Callitrichaceae, <i>Isoetes lacustris</i> , Nymphaeaceae)	Facies indicator (water-table level)
Pm	Asteroideae, Cichorioideae, Fabaceae, Poaceae	Indicator of vegetation physiognomy
M	Mediterranean taxa (mainly <i>Quercus ilex</i> ; sporadic <i>Pinus halepensis</i> and <i>P. pinea</i> )	Facies + climate indicator (climate optimum)
Q+ other DT	Mixed oak forest and accessory taxa ( <i>Carpinus betulus</i> , <i>Corylus avellana</i> , <i>Fraxinus excelsior</i> , <i>Ostrya carpinifolia</i> , <i>Quercus cerris</i> , <i>Q. pubescens</i> , <i>Q. robur</i> , <i>Tilia</i> , <i>Ulmus</i> )	Facies + climate indicator (climate optimum)
Mt	Mountain taxa ( <i>Abies alba</i> , <i>Alnus incana</i> , <i>Alnus viridis</i> , <i>Castanea sativa</i> , <i>Dryas octopetala</i> , <i>Fagus sylvatica</i> , <i>Picea excelsa</i> , <i>Pinus mugo</i> , <i>Pinus</i> sp.-to be discussed, Saxifragaceae).	Climate indicator (cool climate)
Alia	Ubiquitous taxa + As group (anthropic spontaneous), the latter including <i>Bellis perennis</i> , <i>Centaurea nigra</i> and <i>Tussilago farfara</i> (Asteroideae) and Chenopodiaceae, Plantaginaceae, Polygonaceae, <i>Spergula arvensis</i> , and Urticaceae	Local disturbed environment

*Hygrophyte plants (Hyg)*: this group includes woody taxa that can tolerate only short periods of drowning (*Alnus glutinosa*, *Populus* and *Salix*) and herbs that indicate general humid conditions (Cyperaceae and most Pteridophytes). It mainly accounts for hygrophilous woods and related canopy clearings. Correspondent PDBs are Aw and Ww, both including several herbaceous hygrophytes and aquatics.

*Aquatic plants (Aq)*: this group includes many types of plants (helophytes and hydrophytes) that grow in swampy environments adjacent to hygrophilous woods (Aw, Ww and Swh biomes). Helophytes, including *Butomus umbellatus*, *Isoetes durieui*, *I. hystrix* and various Typhaceae, can tolerate long periods of drowning and, therefore, live with the sole radical apparatus immersed. Hydrophytes consist, instead, of fully aquatic plants (mainly Callitrichaceae, *Isoetes lacustris*, Nymphaeaceae and *Sparganium emersum*) that live in water, either floating or immersed.

*Pasture meadow (pm)*: this group mainly comprises Fabaceae and undetermined Asteroideae, Caryophyllaceae, Cichorioideae and Poaceae. Their attribution to biomes Phg and Dg is consistent with their ecological characteristics, as a variety of different herbs can colonise temporarily-emerged areas (e.g.: Caryophyllaceae from seaward localities, Poaceae from a very wide range of different environments, Cichorioideae and Asteroideae from pastures).

*Mediterranean taxa (M)*: this group mainly consists of *Quercus ilex* (falling into the Mo-ho biome) with the negligible presence of *Erica*, *Helianthemum*, *Pinus nigra* and *P. pinea*, which for this reason were not considered for elaborating PDBs (i.e., occasional taxa).

*Quercus + other Deciduous trees (Q+other DT)*: this includes all deciduous oak taxa (*Quercus cerris*, *Q. pubescens*, *Q. robur* and *Quercus undiff.*), as well as other deciduous trees (*Carpinus betulus*, *Corylus avellana*, *Fraxinus excelsior*, *F. ornus*, *Ostrya carpinifolia*, *Tilia cordata*, *T. platyphyllos* and *Ulmus minor*) that compose the Po Plain PNV. Deciduous oak taxa (with the exception of *Q. robur*) fall into the holm oak-mixed oak biome (instead of the mixed oak), in an ecological subordinate to coordinate position with *Q. ilex*. This suggests remarkable influence of the coastal holm oak – mixed oak forest on the local environment. The attribution of *Q. robur* and *Fraxinus excelsior* to the Montane humid vegetation biome (Fig. 3) is because the sub-Mediterranean vegetation belt in ER extends up to 800 m a.s.l. (Ferrari, 1997; Pignatti, 1998).

*Montane taxa (Mt)*: given the remarkable distance (ca. 50 km) of the core site from the Apennines, all taxa ranging in height a.s.l. from the Beech woods to the Ericaceous shrublands above the timberline were incorporated into this group. These taxa include all Conifers (*Abies alba*, *Picea excelsa* and *Pinus mugo*), montane broadleaves (*Alnus incana* and *A. viridis*) and herbs (*Dryas octopetala* and various Saxifragaceae), mainly belonging to both montane biomes (Fig. 3). *Artemisia* was not included because of uncertainties in species determination and ecology (Pignatti, 1982; Subally and Quézel, 2002). Though *Pinus* sp. falls within the mixed oak forest biome (Fig. 3), it was interpreted as part of the regional (sub-regional) pollen rain for the following reasons: *i*) temperate pine taxa, such as *P. halepensis*, *P. nigra* and *P. pinea*, were found in negligible amounts (<1%) in very few samples only, *ii*) *Pinus* sp. pollen was never found in concentrations high enough to depict the onset of any pine wood, such as the one that colonized the Po Plain during the Preboreal and declined throughout the Boreal (Ferrari et al., 1997; Accorsi et al., 1999, 2004), and *iii*) *Pinus* sp. variations mainly follow those of the other taxa grouped into the *Mt* pollen group. *Abies alba* also falls into the mixed oak forest biome; in this case, its retrieval in the same branch of *Tilia cordata* and *T. platyphyllos* likely indicates its preference for relatively moist conditions, both in mountainous and lowland areas.

*Alia*: this group includes all taxa excluded from previous groups (ubiquitous taxa and others belonging to *As* - Anthropogenic spontaneous). Specifically, several Asteroideae (*Bellis perennis*, *Centaurea nigra* and *Tussilago*

*farfara*), Caryophyllaceae (*Spergula arvensis*), Papaveraceae, Plantaginaceae, Polygonaceae and Urticaceae characterise this group.

In sum, according to cluster analysis (Fig. 3) all pollen groups bear a more or less marked facies signal. Only the montane taxa group can be considered a true “outsider”, an indicator of regional/sub-regional (Po Plain and surrounding reliefs) vegetation, being represented by taxa that never colonised the coastal/delta plain during the current interglacial. Thus, if stratigraphically plotted, increasing *Mt* percentages can allow the identification of climate-driven altitudinal variations on plant communities (i.e., expansions of mountain vegetation belts). Relative abundances of the identified pollen groups are reported in Fig. 4 (pollen spectra), while relative concentrations of the main taxa composing each group are reported in Figs. 5-6.

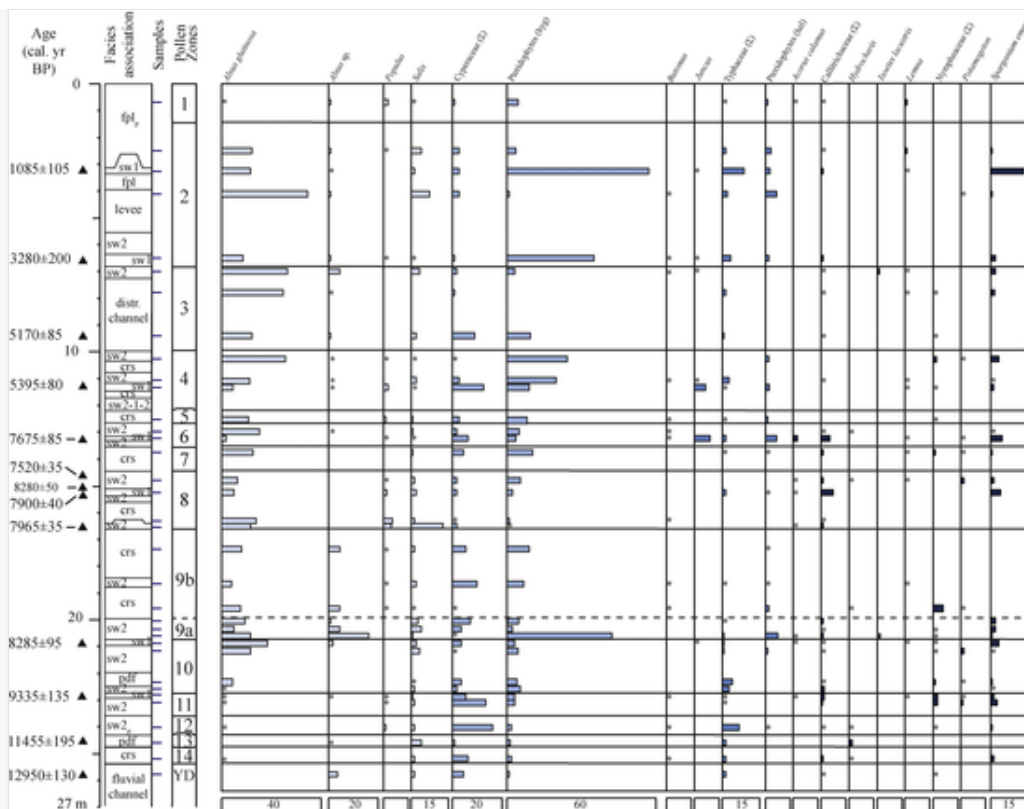
alt-text: Fig. 4

Figure 4. Fig. 4









Pollen percentage diagram, showing the relative abundances of hygrophytes (woody and herbaceous) and aquatics (helophytes and hydrophytes), both considered good facies indicators in terms of local humidity and water table level. Asterisk represents percentages < 1%. Facies abbreviations: distributary channel (distr. channel), crevasse splay (crs), poorly drained floodplain (pdf), fpl (floodplain), swamp 2 (sw2), swamp 1 (sw1); the “p” subscript means pedogenised.

#### 4.2.4.2 Depositional facies associations

Five main facies associations (floodplain, swamp1, swamp2, overbank/crevasse and distributary channel deposits in Fig. 4) were identified combining sedimentological and palynological data derived from the local pollen rain (Table 2). Each facies association shows particular and rather uniform vegetation communities ( Figs. 4-6) defined by taxa living in the alluvial plain. The floodplain facies association (silt and clay with Fe—Mn oxides and carbonate nodules) is characterised by the dominance of pasture-meadows (ca. 14–48%) over hygrophytes and aquatics (<10% and <8%, respectively), pointing to a low degree of hygrophily. By contrast, swamp2 deposits (organic-rich clay) show the highest percentages (10–77%) of hygrophytes accompanied by low values of aquatics (5–11%), indicating a submerged environment with a relatively low level of the water table. The highest groundwater level characterises peat-rich swamp1 deposits, where *Aq* shows the highest percentages (9.6–32%), similar to *Hyg*. Sandy overbank/crevasse and distributary channel deposits contain relatively high abundances of hygrophytes (up to 25%), thus documenting hygrophily. More detailed palynological and sedimentological features of facies associations are reported in Table 3.

alt-text: Table 3

Table 3: Table 3



The presentation of Tables and the formatting of text in the online proof do not match the final output, though the data is the same. To preview the actual presentation, view the Proof.

Diagnostic sedimentological and palynological features of the main facies associations from the Holocene succession of core EM2.

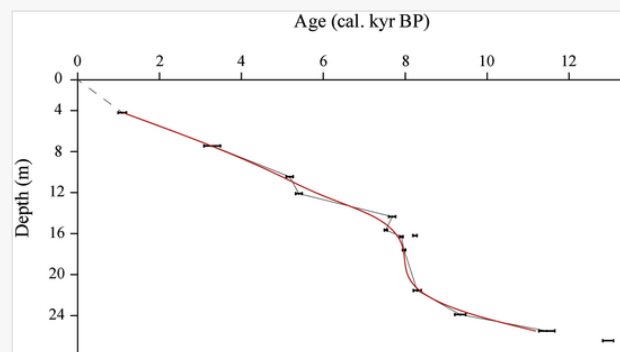
Facies association	Sedimentological features	Palynological content
Peaty swamp (sw1)	Black to dark brown peat, 10 to 30 cm-thick	Arboreal cover shows low values, ranging between 10– <del>and</del> 47%. The <i>Aq</i> group shows the highest percentages (9.6–32%); both <i>Q</i> <sub>1</sub> + <i>other DT</i> and <i>M</i> groups display low percentages (ca. 7% and 5%, respectively). Among woody hygrophytes, <i>Alnus glutinosa</i> is the dominant tree (ca. 8%). The <i>pm</i> group, mainly composed by Poaceae, occurs with relative abundances ranging between 11– <del>and</del> 49%
Swamp (sw2)	Grey to dark grey clays-silty clays, high but variable amount of decomposed organic matter and plant remains	The <i>Hyg</i> group shows high percentages (10–77%) with the dominance of <i>Alnus</i> ( <i>A. glutinosa</i> and <i>A. undiff.</i> ), Cyperaceae and Pteridopythes, locally accompanied by <i>Salix</i> and <i>Populus</i> . The <i>Aq</i> group occurs with percentages ranging between 5– <del>and</del> 11%, while the <i>Q</i> <sub>1</sub> + <i>other DT</i> and <i>M</i> show a high range of variability (6–34% and 2–24%, respectively). <i>Pm</i> , commonly represented by Poaceae and subordinate Cichorioideae and Asteroideae, occurs with percentages that vary between 7– <del>and</del> 41%
Floodplain/Poorly drained floodplain (fpl/pdf)	Light grey to grey clay-silty clay and grey to brown silty clay-sandy silt. Local presence of calcareous nodules and Fe—Mn oxides, plant remains and a variable amount of decomposed organic matter	The pollen assemblage is heterogeneous with remarkable percentages of the <i>pm</i> group (ca. 14–48%), while <i>Aq</i> commonly occurs with abundances lower than 8%. <i>Hyg</i> is well represented (ca. 10–27%) with <i>Salix</i> as a significant component. <i>Q</i> <sub>1</sub> + <i>other DT</i> and <i>M</i> show highly variable percentages between 1– <del>and</del> 37%
Crevasse splay/Levee (crs, lev)	Silty sand to sandy silt deposits, dm to few m-thick, organised in alternating layers (lev) or coarsening-upward (crs) successions. Scattered plant fragments and Fe—Mn oxides	The arboreal cover is generally high (51–77%). The <i>Hyg</i> dominates (i.e., <i>Alnus glutinosa</i> , <i>Salix</i> , Cyperaceae and Pteridophytes) and reach abundances of ca. 25%, while <i>pm</i> commonly stands around 12%. Various taxa belonging to <i>Q</i> <sub>1</sub> + <i>other DT</i> and <i>M</i> occur with percentages that vary around 7 and 20%, respectively
Distributary channel (dch)	M-thick (ca. 3 m), medium to fine sandy succession. Erosional lower boundary and scattered wood fragments	Remarkable occurrence of taxa belonging to <i>Hyg</i> and <i>Aq</i>

### 4.3.4.3 Chronology

The age model (Fig. 7) indicates that the studied succession above the thick fluvial sand body covers the whole Holocene (Table 1; Figs. 2, 4). In general, most radiocarbon dates are stratigraphically coherent, with very few exceptions. Stratigraphic reversal was observed at ca. 15 m core depth, possibly reflecting reworking of older plant remains, and the related sample was discarded. Eleven out of twelve radiocarbon ages (2-sigma calibrated years BP) were interpolated using a smoothing spline function omitting the age of ca. 12,950 cal yr BP as it belongs to the abandonment facies of a fluvial channel belt (Fig. 4), whose sedimentation rates are unclear. The resulting age-depth model suggests that three main stratigraphic intervals, reflecting rather constant sedimentation rates, can be identified (Fig. 7). The lowermost interval (ca. 11.7–8.3 cal ky BP) denotes an accumulation rate of ca. 1.4 mm/yr. Upwards, between ca. 8.3–7.7 cal ky BP, the accumulation rate strongly increases up to ca. 10 mm/yr. Its value drops to about 1.5 mm/yr between 7.7 and 1.1 cal ky BP, though the presence of a distributary-channel deposit around 10 m partly lowers this estimation. The wood fragment sampled at the base of the channel deposit and dated to around 5.2 kyr BP probably derives from the underlying eroded swamps. Thus, this age should be considered as a *terminus post-quem*. The uppermost 3 meters of the cored succession, younger than 1085 years BP, have a more uncertain chronology due to the lack of radiocarbon dates.

alt-text: Fig. 7

Figure 7: Fig. 7



Core EM2 age-depth model obtained applying the smoothing spline function (red line; smooth value = 0.85) using the software PAST (Hammer et al., 2001). The thin black line shows the linear interpolation among ages. Radiocarbon ages are listed in Table 1. (For interpretation of the references to colour in this figure legend, the reader is referred to the web version of this article.)

#### 4.4.4.4 Vegetation phases

Opportunely framed into a high-resolution chronological-facies context, the relative proportion of *Mt* relative to *Q* + other *DT* and *M* allows the identification of 14 pollen zones (PZs, Fig. 4). Considering montane taxa as a good proxy for climate degradation and mixed oak-holm oak forest trees as indicators of the local achievement of the vegetation final stage (Table 2), PZs were grouped into five main vegetation phases. They are described in ascending order.

PZs 14–11 (ca. 25.50–23 m; <12,950–9300 cal. yr BP): this interval overlies a tens m-thick alluvial succession mainly formed by fluvial-channel sands (i.e., Po channel belt) and overbank deposits constrained to

the last glacial period (Fig. 4 – Amorosi et al., 2017b). The uppermost portion of the channel fill probably developed under Lateglacial conditions (Cacciari et al., 2018), characterised by the remarkable abundance of *Mt* (ca. 13.5%, with *Pinus mugo* up to 5.9%). An abrupt vegetation change is recorded within PZ 14, where montane taxa decrease (ca. 6.9%) and *Quercus ilex* appears in significant amounts (4.7%), marking the onset of the Holocene. As a whole, relative abundances of *Q*+*other DT* and *M* (ca. 7% and 5%, respectively) compared to that of *Mt* (ca 10%) point to an early stage of vegetation development. PZs 13 and 11 record two short-term changes in the plant community, irrespective of the facies signal. PZ 13 is characterised by a slight increase in montane taxa, which is paralleled almost by the disappearance of the mixed oak and Mediterranean taxa. By contrast, a more pronounced enrichment of *Mt* (up to 15.8%) occurs within PZ 11.

*PZ 10* (ca. 23–21 m; ca. 9300–8300 cal. yr BP): even though local driving factors, mainly highlighted by aquatics and hygrophytes, may have affected the plant community, this interval records a sudden decrease in montane taxa, which are almost totally replaced by Mediterranean and deciduous broadleaves. Specifically, *Mt* drops to a minimum value of 1%, whereas *M* and *Q*+*other DT* peak around 26% and 37%, respectively, marking the achievement of the PNV on the plain.

*PZs 9–7* (ca. 21–13.5 m; ca. 8300–7700 cal. yr BP): this interval records a period of high-frequency variability in the vegetation community that encompasses several facies in the record. Its lowermost portion (PZ 9, ca. 8285–8000 cal. yr BP) shows a pronounced peak in montane taxa (14–24%) that is paralleled by a decrease in Mediterraneans, while the mixed oak forest remains well represented. Upwards, PZ 8 documents the recovery of holm oak forests accompanied by a sharp decline in montane taxa. The observed concentration of *Quercus ilex* (6–10%) is also considered significant because of the locally high water-table. This interval shows an upward expansion of montane trees (ca. 22%, PZ 7).

*PZs 6–3* (ca. 13.5–7 m; ca. 7700–3700 cal. yr BP): the pollen content in this interval documents high-frequency changes in vegetation communities less pronounced than in underlying PZs 9–7. Two events of *Mt* expansion (PZs 5 and 3) interrupt a pollen spectrum indicative of a mesic holm oak-mixed oak forest developed laterally to hygrophilous prairies and herbaceous wetlands (PZs 6 and 4). Specifically, PZ 5 exhibits a high concentration of *Mt* (ca. 26%) showing almost all taxa found in the studied succession (except for *Pinus sylvestris*) and accompanied by most of broadleaves. A relative increase in montane taxa is also recorded within the PZ 4, but it is not paralleled by a significant drop in Mediterraneans.

*PZs 2–1* (uppermost 7 m; <3700 cal. yr BP): pollen data in PZ 2 point to the establishment of a holm oak-mixed oak forest without a significant peak in *Mt*. A peculiar pollen assemblage indicative of a disturbed environment with a strong reduction in forest cover to the benefit of *pm* (mainly Cichorioideae) and a remarkable peak in montane taxa are found within PZ 1.

## 5.5 Discussion

### 5.1.5.1 Holocene vegetation and climate dynamics

#### 5.1.1.5.1.1 The onset of the Holocene (ca. 11.7–9.3 kyr BP)



The beginning of the Holocene (PZ 14 in Fig. 4) is marked by the appearance of *Quercus ilex*, accompanied by mixed oak-holm oak elements, suggesting the establishment of particularly favourable microclimatic conditions in the coastal plain. This interpretation is strengthened by very low percentages of *Pinus* sp., compared to the coeval *Pinus sylvestris* forest developed in the Po Plain (Accorsi et al., 1999, 2004; Valsecchi et al., 2011). A partially coeval (12000–11,700 cal yrs. BP) rapid expansion of a mixed open broadleaved forest has been recorded at Lake Ledro (southern Alps, Italy), Lake Fimon (23 m a.s.l., N Italy) and within marine deposits of the South Adriatic Sea (Valsecchi et al., 2011; Combourieu-Nebout et al., 2013; Joannin et al., 2013). An increasing trend in species richness and in the relative abundance of mixed oak-holm oak taxa, which probably reflects the vegetation response to progressively increasing temperature and precipitation, is interrupted by two peaks in montane taxa dated to around 11,400 cal yr BP and 9300 cal yr BP (PZs 13, 11 in Fig. 4). PZ13 is characterised by the strong decline of mixed oak-holm oak forests, mainly for the benefit of *Alnus viridis*, accompanied by low amounts of *Pinus mugo*, *Betula* and *Castanea*, highlighting a cool-wet climate ascribable to the Preboreal oscillation (PBO/Bond event 8; ca. 11,300–11,100 cal BP, Bond et al., 1997; Rasmussen et al., 2007a, 2007b, 2014). Interestingly, this cool and wet phase shows similar vegetation dynamics to those reconstructed in NE Europe (De Klerk et al., 2006) and the Netherlands (Bos et al., 2007), whereas cool and dry conditions commonly characterise the PBO event in the Mediterranean record (e.g.: Lake Trifoglietti and Lake Accesa in southern and central Italy, respectively, and in several marine cores - Dormoy et al., 2009; Favaretto et al., 2009; Magny et al., 2013). The youngest (PZ11) peak in montane taxa suggests another episode of climate cooling consistent with the Boreal oscillation (Rasmussen et al., 2007a, 2007b, 2014). It is marked by a general increase in conifers (*Abies*, *Picea* and *Pinus mugo*, with *Pinus* sp. in the background), although no montane alders and no *Quercus ilex* decrease are observed. These features suggest less cool but drier conditions than during the PBO.

### 5.1.2.5.1.2 Early-mid Holocene optimum and the 8.2 ka event (ca. 9.3–7.7 kyr BP)

The abrupt expansion of mixed oak-holm oak forests on the plain around 9300 cal yr BP (PZ 10; Fig. 4) marks the rapid establishment of the PNV corresponding to the beginning of the Holocene climate optimum. Within the uppermost part of PZ 10, holm oak-mixed oak taxa are partially replaced by hygrophytes, reflecting the establishment of a hygrophilous vegetation under similar climate conditions, but in a different environment. Warm temperate oak forests characterize the latest Boreal and the early Atlantic landscape of the Po Plain (PZs 10–7), as documented by several on-land pollen records from both sides of the Adriatic (Watts et al., 1996; Jahns and van der Bogaard, 1998; Sadori et al., 2011). However, two short-term periods of climate worsening occurred at the early-mid Holocene transition (*Mt* peaks around 8300–8000 cal yr BP and 7700 cal yr BP). The former has an impressive stratigraphic evidence (ca. 3 m in 300 years) that allows the detailed reconstruction of vegetation dynamics during the well-documented 8.2 ka cooling event-Bond event 5 (Bond et al., 1997; Rasmussen et al., 2007a, 2007b, 2014):

- i) firstly, *Alnus incana*, *A. viridis* and *Fagus sylvatica* appeared (PZ 9a), documenting the expansion of the regional hygrophilous montane vegetation, probably favoured by slightly cooler and wetter conditions (Figs. 4, 5);
- ii) shortly after *F. sylvatica* disappeared, giving way to *Abies* and *Picea*, while *A. incana* and *A. viridis* significantly increased (PZ 9b; Figs. 4, 5). These two events document the first



destabilization of the montane vegetation community and further enhancement of the annual rainfall, respectively. Our interpretation is also supported by the high variability in local re-colonisation processes, which saw different broadleaves competing for the same strongly disturbed environment (Fig. 5). Accordingly, an antagonistic behaviour of *Fagus sylvatica* and *Abies* is recorded at Lake Ledro (N Italy), where an expansion of *Abies* occurred around 8.2 ka (Joannin et al., 2013).

The second peak in montane taxa (PZ 7) shows the remarkable abundance of *Pinus mugo* (ca. 9.3%; Fig. 5), which almost completely replaced the other conifers. Although these features indicate a further degradation in high altitude vegetation communities and a possible lowering of the timberline, framing this event into a wider climate context is complicated. For the south Adriatic, Combourieu-Nebout et al. (2013) identified a short-term phase of holm oak-mixed oak forest decrease at 7.9–7.6 kyr BP, accompanied by a peak in *Abies* and *Picea*, both rapidly replaced by *Pinus*. This vegetation change was interpreted to reflect increased precipitations and lower temperatures. Interestingly, the previous decline in *Quercus* pollen is dated to around 8.3–8.2 kyr BP and linked to a decrease in temperature, which leads to the hypothesis of a local (Adriatic?) complex expression of the ‘8.2 ka event’. In our record this climate feature is clearer, possibly due to the influence of Siberian High outbreaks (Bora wind) on the northern Adriatic area. Indeed, Bora is a winter downslope wind that blows from the Pannonian plain through the lower portions of the Julian and Dinaric Alps into the north and central Adriatic Sea (Signell et al., 2010). Since seasonality increases during periods of climate cooling, Bora wind could also become stronger, enhancing pollen transportation from the alpine Oroboreal Conifer forest belt (*P. mugo* and *Picea* occupy the present-day shrublands above the timberline of the southern Alps; Ferrari, 1997), as well as from the Apennines (*Alnus viridis* in Mercuri, 2015) down to the Po Plain.

### 5.1.3.5.1.3 Mid Holocene optimum and transition to the late Holocene (ca. 7700–3700 cal yr BP)

After the perturbation centred at 7700 cal yr BP, the return to climate optimum conditions is recorded by the hygrophilous version of PNV, which characterised the Po Plain landscape up to ca. 5000 cal yr BP (late Atlantic). However, a short-lived, marked peak in montane taxa (PZ 5 in Fig. 4) points to a minor climate cooling centred on 7000 cal yr BP. Although a semi-coeval climate change has been patchily recorded within the Mediterranean marine record (Fletcher and Zielhofer, 2011; Combourieu-Nebout et al., 2009, 2013; Desprat et al., 2013), our data show an impressive and peculiar tree species diversity (including *Q*+*other DT*), suggesting low impact of this climate oscillation on the vegetation cover. A further minor increase in montane trees occurs between ca. 5000–3800 cal yr BP (PZ 3; Fig. 4). In this instance, the absence of *Abies*, *Fagus* and *Picea* coupled with the high degree of chronological uncertainty due to the presence of an erosional distributary channel, prevent from in-depth palaeoclimate reconstructions.

### 5.1.4.5.1.4 Late Holocene (last 3700 years)

According to Accorsi et al. (1999, 2004), the late Holocene pollen record of the Po Plain (PZs 2–1; Fig. 4) documents the development of a vegetation landscape characterised by hygrophilous forests and by a clear shrinking of the holm oak and mixed oak woods, probably related to a heavier human land-use. Moreover, a peak of *Q. ilex* accompanied by a mixed oak forest recovery dated to around 830 cal. yr BP (Fig. 4) could

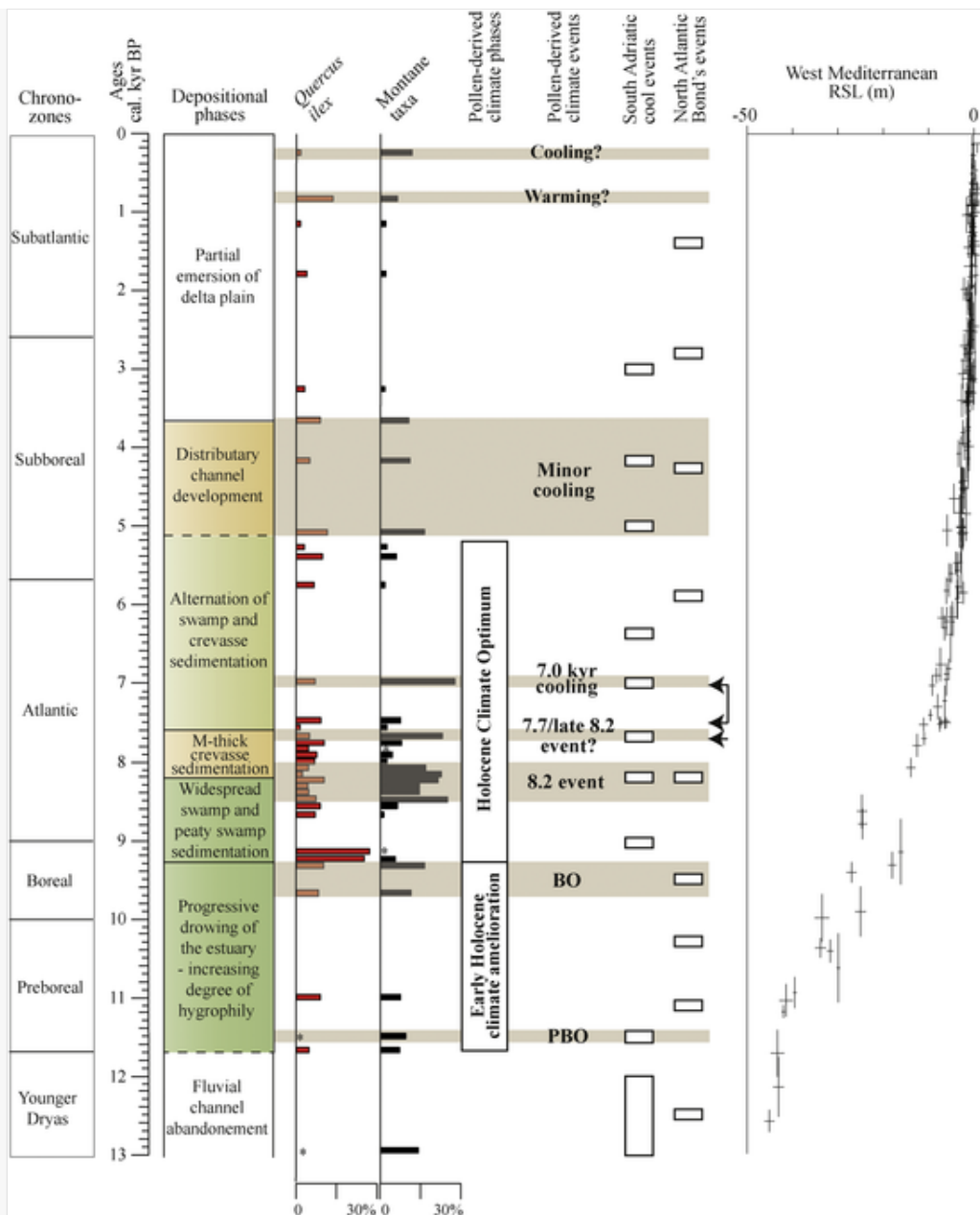
represent the Medieval Climate Optimum. The following increase in montane taxa exclusively represented by *Pinus* species could be related to the Little Ice Age.

### 5.2.5.2 Climate imprint on landscape evolution and depositional patterns

The main shifts in Holocene vegetation, reconstructed from pollen data, fit well key depositional and palaeoenvironmental changes in the Po Plain (Fig. 8). This suggests a primary role of climate fluctuations, in addition to glacio-eustatic changes (MWPs-Melt Water Pulses), in shaping the coastal landscape. The marked warming documented by the appearance of *Q. ilex* corresponds to a phase of general drowning of the Po estuary (Figs. 2, 8; Bruno et al., 2017), revealing a simultaneous vegetation-depositional response at ca. 11.7 cal kyr BP under combined climate and eustatic forcing factors related to MWP 1B (Fairbanks, 1989; Vacchi et al., 2016). In the earliest Holocene (before 9.3 cal kyr BP), the increasing degree of hygrophily (overbank/crevasse deposits overlain by swamps; Fig. 4) reflects the landward migration of facies under the predominant forcing of relative sea-level (RSL) rise (Vacchi et al., 2016). In this context, high-frequency events of climate cooling revealed by peaks in montane taxa (e.g., PBO and BO) do not seem to affect significantly coastal depositional patterns (Fig. 8). Interestingly, a generalized phase of flooding that led to a widespread peaty sedimentation in the area (Bruno et al., 2017) is concomitant with the establishment of optimum climate conditions, marked by the PNV achievement (Fig. 8). During this period, the inner portion of the estuarine system appears to be particularly sensitive to cooling episodes (centred at ca. 8.2, 7.7 and 7.0 cal kyr BP). Indeed, increased fluvial activity led to the rapid sedimentation of thick crevasse splay sands and silts fed by a nearby distributary channel (Fig. 2) and intercalated with peaty swamp and swamp clays (average accumulation rate of ca. 6 mm/yr between 8.3- and 7.0 cal kyr BP). A marked peak in river floods has been documented by Benito et al. (2015a, 2015b) for the entire Mediterranean area between ca. 8000-7000 cal yr BP. Increased river inputs have been identified in the Adriatic Basin and correlated to the 7.7 and 7.5-7.0 cal kyr BP climate events (Combourieu-Nebout et al., 2013). Moreover, enhanced flood activity dated ca. 8.2-7.1 cal kyr BP was identified by Zhornyak et al. (2011) in the Apuan Alps (Renella cave, NW Italy). These combined climate-stratigraphic data suggest that major shifts towards enhanced fluvial activity possibly reflect phases of increased soil erodibility related to climate-driven changes in vegetation cover, as already hypothesized by Fletcher and Zielhofer (2013).

alt-text: Fig. 8

Figure 8: Fig. 8



Comparison between depositional dynamics (vertical stacking pattern of facies), pollen-derived climate phases and climate events recorded in core EM2. Palynological samples are plotted against time instead of depth (Figs. 4-6) applying the age-depth model reported in Fig. 7; unique exception is the sample centred at 11.7 cal kyr BP, as its chronological attribution is based on the pollen content (i.e., remarkable appearance of *Q. ilex*). Chronozones of Mangerud et al. (1971), slightly modified by Ravazzi (2003), and cooling events recorded in the North Atlantic area (Bond's events; Bond et al., 1997) and the south Adriatic Sea (Combourieu-Nebout et al., 2013) are also highlighted. Black arrows indicate phases of enhanced runoff of Po and Adriatic rivers, as reported by Combourieu-Nebout et al. (2013). Plots of RSL index points from western Mediterranean (Vacchi et al., 2016) are also shown. PBO: Preboreal Oscillation; BO: Boreal Oscillation.

The stratigraphically expanded sedimentary record of the Po estuary also allows the examination of depositional dynamics and their relation to vegetation patterns on sub-millennial time scales around the well-known 8.2 ka event (Fig. 8). The onset of a cooler climate is testified by the sudden appearance, among montane taxa, of *Fagus sylvatica*, within peaty swamp deposits dated to around 8300 cal yr BP. Following a further step of montane forests degradation (*F. sylvatica* is replaced by *Abies alba*; Fig. 5), the depositional

system reacts via increased fluvial (crevasse) sedimentation. These dynamics suggest a different response of coastal sedimentation compared to the vegetation community, as this latter exhibits an almost immediate response to climate cooling. By contrast, a time lag is not observed for the subsequent cooling phase centred at 7.7 cal kyr BP that possibly records a second spell of the 8.2 ka event (Figs. 4, 8).

The end of climate optimum conditions and the transition to the late Holocene (ca. 5000–3700 cal yr BP) are locally recorded by a 3 m-thick distributary-channel sand body, which is part of a complex drainage network that fed the Po delta plain during the earliest phases of progradation (Amorosi et al., 2017a, 2019). Although this stratigraphic interval is affected by a low palynological-chronological resolution due to the sandy nature of the deposit (Figs. 7, 8), our record of enhanced fluvial activity is well correlated with a major Po River avulsion and the consequent reorganization of the deltaic network reported for the same period of time (Rossi and Vaiani, 2008; Piovani et al., 2012; Amorosi et al., 2017a, 2017b). This phase was also contemporaneous to widespread deforestation induced by transhumant pastoralism during the Eneolithic (Cremaschi and Nicosia, 2012; Bruno et al., 2015)

## 6.6 Conclusions

The combined palynological and stratigraphic analysis of the Holocene depositional record from the subsurface of the modern Po delta-coastal plain (core EM2) enables differentiation of environmental (local) and climate (regional) changes, both marked by distinctive vegetation dynamics, in a key area between the continental and marine realms. Placed within a robust facies and chronological framework, shifts in vegetation communities from stratigraphically expanded (tens m-thick), organic-rich deposits that accumulated in inner estuarine-deltaic settings provide high-resolution (millennial-scale) data about Holocene palaeoclimate variations in the N Adriatic area. The major outcomes of this study can be summarised as follows:

- Nine pollen-derived biomes (PDBs) were identified from the core EM2 pollen record through cluster analysis. The resulting dendrogram mainly reflects the development of different vegetation communities under optimum conditions (PNV) and along environmental-local humidity/disturbance gradients.
- The comparison between PDBs, local present-day vegetation belts and (auto)ecological features of the identified taxa allowed us to define seven pollen groups and to interpret them in terms of environmental and/or climate forcing. Only montane taxa (*Mt*) exclusively reflect the regional/sub-regional pollen rain, whereas Mediterranean (*M*) and deciduous broadleaved (*Q* + *other DT*) taxa are indicative of PNV on the plain.
- Stratigraphic variations in montane taxa document changes in the altitudinal distribution of vegetation communities linked to cooling periods. This vegetation-climate variability fits well with Bond events, especially for the early-mid Holocene, suggesting a strong Mediterranean–North Atlantic climate link at high-frequency time intervals.
- One major vegetation change (dated between 8.3–and 8.0 cal kyr BP) coincides with the widespread climate perturbation attributed to the 8.2 ka cooling event.
- Climate played a major role in shaping coastal landscapes in addition to glacio-eustatic

variations, determining changes in the local and regional vegetation cover, as well as triggering an increase in fluvial activity.

Supplementary data to this article can be found online at <https://doi.org/10.1016/j.palaeo.2019.109468>.

## Uncited references

[Allen et al., 2002](#)

[Bond et al., 2001](#)

[Vescovi et al., 2018](#)

[Walker et al., 2018](#)

## Declaration of competing interest

The authors declare that they have no known competing financial interests or personal relationships that could have appeared to influence the work reported in this paper.

## Acknowledgements

MC acknowledges funding from the Marco Polo Programme (University of Bologna) for research mobility and fruitful collaborative research work. This research was possible thanks to a collaborative research project supported by ExxonMobil Upstream Research Company (grant to A. Amorosi) and to collaboration with the team of palynologists and archaeobotanists at “*Centro Agricoltura e Ambiente G. Nicoli*” laboratory (Italy). We are grateful to N. Marriner for the English language editing and revision, and to M. Vacchi for providing the high-resolution image of W Mediterranean RSL index points. A special thank goes to C. Ferrari, who provided several interesting papers on ER regional vegetation, and to A. Chiarucci, who deepened our knowledge of the PNV concept. We are also very thankful to the reviewers and Editor, who provided careful reviews of the manuscript and greatly improved it through their comments and remarks.

## References



The corrections made in this section will be reviewed and approved by journal production editor.

Accorsi, C.A., Bandini Mazzanti, M., Forlani, L., Mercuri, A.M., Trevisan Grandi, G., 1999. An overview of Holocene forest pollen flora/vegetation of the Emilia Romagna region – Northern Italy. *Archivio Geobotanico* 5 (~~1-2~~1-2), 3–27.

Accorsi, C.A., Bandini Mazzanti, M., Forlani, L., Mercuri, A.M., Trevisan Grandi, G., 2004. Holocene forest vegetation (pollen) of the Emilia Romagna plain – northern Italy. In: Pedrotti F, Gehu J.M. (eds)

La végétation postglaciaire du passé et du présent. Syngenèse, synécologie et synsystème. Colloq. Phytosociol. 28, 1–103.

Allen, J.R.M., Watts, W.A., McGee, E., Huntley, B., 2002. Holocene environmental variability – the record from Lago Grande di Monticchio, Italy. *Quat. Int.* 88, 69–80.

Amorosi, A., Colalongo, M.L., Fiorini, F., Fusco, F., Pasini, G., Vaiani, S.C., Sarti, G., 2004. Palaeogeographic and palaeoclimatic evolution of the Po Plain from 150-ky core records. *Global Planet. Change* *Glob. Planet. Chang.* 40, 55–78.

Amorosi, A., Dinelli, E., Rossi, V., Vaiani, S.C., Sacchetto, M., 2008. Late Quaternary palaeoenvironmental evolution of the Adriatic coastal plain and the onset of the Po River Delta. *Palaeogr. Palaeoclimatol. Palaeoecol.* 268, 80–90.

Amorosi, A., Maselli, V., Trincardi, F., 2016. Onshore to offshore anatomy of a Late Quaternary source-to-sink system (Po Plain – Adriatic Sea, Italy). *Earth-Sci. Rev.* 153, 212–237.

Amorosi, A., Bruno, L., Campo, B., Morelli, A., Rossi, V., Scarponi, D., Hong, W., Bohacs, K.M., Drexler, T.M., 2017. Global sea-level control on local parasequence architecture from the Holocene record of the Po Plain, Italy. *Mar. Petroleum Geol.* 87, 99–111.

Amorosi, A., Bruno, L., Cleveland, D.M., Morelli, A., Hong, W., 2017. Paleosols and associated channel-belt sand bodies from a continuously subsiding late Quaternary system (Po Basin, Italy): new insights into continental sequence stratigraphy. *Geol. Soc. Am. Bull.* 129 (3–4), 449–463.

Amorosi, A., Barbieri, G., Bruno, L., Campo, B., Drexler, T.M., Hong, W., Rossi, V., Sammartino, I., Scarponi, D., Vaiani, S.C., Bohacs, K.M., 2019. Three-fold nature of coastal progradation during the Holocene eustatic highstand, Po Plain, Italy – close correspondence of stratal character with distribution patterns. *Sedimentology* doi:10.1111/sed.12621.

Badino, F., Ravazzi, C., Valié, F., Pini, R., Aceti, A., Brunetti, M., Champvillair, E., Maggi, V., Maspero, F., Perego, R., Orombelli, G., 2018. 8800 years of high-altitude vegetation and climate history at the Rutor Glacier forefield, Italian Alps. Evidence of middle Holocene timberline rise and Glacier contraction. *Quat. Sci. Rev.* 185, 41–68.

Bard, E., Hamelin, B., Arnold, M., Montaggioni, L., Cabioch, G., Faure, G., Rougerie, F., 1996. Deglacial sea-level record from Tahiti corals and the timing of global meltwater discharge. *Nature* 382, 241–244.

Benito, G., Macklin, M.G., Cohen, K.M., Herget, J., 2015. Past hydrological extreme events in a changing climate. *Catena* 130, 1–108. doi:10.1016/j.catena.2014.12.001.

Benito, G., Macklin, M.G., Panin, A., Rossato, S., Fontana, A., Jones, A.F., Machado, M.J., Matlakhova, E., Mozzi, P., Zielhofer, C., 2015. Recurring flood distribution patterns related to short-term Holocene climatic variability. *Sci. Rep.* 5, 16398. doi:10.1038/srep16398.

Berglund, B.E., Ralska-Jasiewiczowa, M., 1986. ~~Handbook of Holocene palaeoecology and palaeohydrology~~ Handbook of Holocene Palaeoecology and Palaeohydrology. Wiley-Interscience. John Wiley & Sons Ltd, Chichester. ~~1986~~(1986).

Bertoldi, R., 2000. Storia del popolamento vegetale della pianura del Po. In: Ferrari, C., Gambi, L. (Eds.), (a cura di), Un po di terra. Guida all'ambiente della bassa Pianura Padana e alla sua storia. Ed. Diabasis.

Bini, M., Zanchetta, G., Perşoiu, A., Cartier, R., Català, A., Cacho, I., Jonathan, J.R., Di Rita, F., Drysdale, N.R., Finné, M., Isola, I., Jalali, B., Lirer, F., Magri, M., Masi, A., Marks, L., Mercuri, A.M., Peyron, O., Sadori, L., Sicre, M.-A., Welc, F., Zielhofer, C., Brisset, E., 2019. The 4.2 ka BP event in the Mediterranean region: an overview. *Clim. Past* 15, 555–577.

Blasi, C., Capotorti, G., Copiz, R., Guida, D., Mollo, B., Smiraglia, D., Zavattero, L., 2014. Classification and mapping of the ecoregions of Italy. *Plant Biosyst* 148 (6), 1255–1345.

Boccaletti, M., Corti, G., Martelli, L., 2011. Recent and active tectonics of the external zone of the Northern Apennines (Italy). *Int. J. Earth Sci.* doi:10.1007/s00531-010-0545-y.

Bond, G., Showers, W., Cheseby, M., Lotti, R., Almasi, P., deMenocal, P., Priore, P., Cullen, H., Hajdas, I., Bonani, G., 1997. A pervasive millennial-scale cycle in North Atlantic Holocene and glacial climates. *Science* 278, 1257–1266.

Bond, G., Kromer, B., Beer, J., Muscheler, R., Evans, M.N., Showers, W., Hoffmann, S., Lotti-Bond, R., Hajdas, I., Bonani, G., 2001. Persistent solar influence on North Atlantic climate during the Holocene. *Science* 294, 2130–2135.

Bondesan, M., Calderoni, G., Cattani, L., Ferrari, M., Furini, A.L., Serandrei Barbero, R., Stefani, M., 1999. Nuovi dati stratigrafici, paleoambientali e di cronologia radiometrica sul ciclo trasgressivo-regressivo olocenico nell'area deltizia padana. *Annali dell'Università di Ferrara, sezione Scienze della Terra* 8 (1), 1–34.

Bos, J.A.A., Van Geel, B., Van der Plicht, J., Bohnke, S.J.P., 2007. Preboreal climate oscillations in Europe: wiggle-match dating and synthesis of Dutch high-resolution multi-proxy records. *Quat. Sci. Rev.* 26, 1927–1950.

Bronk Ramsey, C., 2009. Bayesian analysis of radiocarbon dates. *Radiocarbon* 51 (1), 337–360.

Bruno, L., Amorosi, A., Severi, P., Bartolomei, P., 2015. High-frequency depositional cycles within the late Quaternary alluvial succession of Reno River (northern Italy). *Ital. J. Geosci.* 134 (2), 339–354.

Bruno, L., Bohacs, K.M., Campo, B., Drexler, T.M., Rossi, V., Sammartino, I., Scarponi, D., Hong, W., Amorosi, A., 2017. Early Holocene transgressive palaeogeography in the Po coastal plain (Northern Italy). *Sedimentology* 64, 1792–1816.



Cacciari, M., Rossi, V., Marchesini, M., Amorosi, A., Bruno, L., Campo, B., 2018. Palynological characterization of the Po delta succession (Northern Italy): Holocene vegetation dynamics, stratigraphic patterns and palaeoclimate variability. In: ~~Alpine and Mediterranean Quaternary 31 (Quaternary: Past, Present, Future – AIQUA Conference, Florence, 13–14/06/2018)~~Alpine and Mediterranean Quaternary 31 (Quaternary: Past, Present, Future – AIQUA Conference, Florence, 13–14/06/2018). pp. 109–112.

Campo, B., Amorosi, A., Vaiani, S.C., 2017. Sequence stratigraphy and late Quaternary paleoenvironmental evolution of the Northern Adriatic coastal plain (Italy). *Palaeogeogr. Palaeoclimatol. Palaeoecol.* 466, 265–278.

Carrión, J.S., Fernandez, S., 2009. The survival of the ‘natural potential vegetation’ concept (or the power of tradition). *J. Biogeogr.* 36, 2202–2203.

Cattaneo, C., 1844. *Introduzione alle notizie naturali e civili sulla Lombardia*. Milano, Bernardoni di Giovanni Tipografo. p. 1844.

Chiarugi, A., 1958. Ricerche sulla vegetazione dell’Etruria. XI: una seconda area relitta di vegetazione di Pigella (*Picea excelsa* Lam.) sull’Appennino Settentrionale. *N. Giorn. Bot. Ital.* 65, 23–42.

Combourieu-Nebout, N., Peyron, O., Domoy, I., Desprat, S., Beaudouin, C., Kotthoff, U., Marret, F., 2009. Rapid climatic variability in the west Mediterranean during the last 25000 years from high resolution pollen data. *Clim. Past* 5, 503–521.

Combourieu-Nebout, N., Peyron, O., Bout-Roumzeilles, V., Goring, S., Dormoy, I., Joannin, S., Sadori, L., Siani, G., Magny, M., 2013. Holocene vegetation and climate changes in the central Mediterranean inferred from a high-resolution marine pollen record (Adriatic Sea). *Clim. Past* 9, 2013–2043.

Correggiari, A., Cattaneo, C., Trincardi, F., 2005. ~~Depositional patterns in the Late Holocene Po delta system. River deltas – Concept, models and examples~~Depositional patterns in the late Holocene Po delta system. River deltas – Concept, models and examples. In: *SEPM Special Publications* 83. pp. 365–392.

Crevaschi, M., Nicosia, C., 2012. Sub-Boreal aggradation along the Apennine margin of the Central Po Plain: geomorphological and geoarchaeological aspects. *Géomorphologie* 2012 (2), 155–174.

Crevaschi, M., Mercuri, A.M., Torri, P., Florenzano, A., Pizzi, C., Marchesini, M., Zerboni, A., 2016. Climate change versus land management in the Po Plain (Northern Italy) during the Bronze Age: new insights from the VP/VG sequence of the Terramara Santa Rosa di Poviglio. *Quat. Sci. Rev.* 136, 153–172.

De Klerk, P., Couwenberg, J., Joosten, H., 2006. Short-lived vegetational and environmental change during the Preboreal in the Biebrza upper basin (NE Poland). *Quat. Sci. Rev.* 26, 1975–1988.

Desprat, S., Combourieu-Nebout, N., Essallami, L., Sicre, M.A., Dormoy, I., Peyron, O., Siani, G., Bout Roumzeilles, V., Turon, J.L., 2013. Deglacial and Holocene vegetation and climatic changes in the

southern Central Mediterranean from a direct land-sea correlation. *Clim. Past* 9, 767–787.

Di Rita, F., Magri, D., 2009. ~~Holocene drought, deforestation and evergreen vegetation development in the central Mediterranean: A 5500 year record from Lago Alimini Piccolo, Apulia, southeast Italy~~Holocene drought, deforestation and evergreen vegetation development in the central Mediterranean: a 5500&nbsp;year record from Lago Alimini Piccolo, Apulia, southeast Italy. *The Holocene* 19, 295–306.

Di Rita, F., Magri, D., 2019. The 4.2 ka event in the vegetation record of the central Mediterranean. *Clim. Past* 15, 237–251.

Di Rita, F., Celant, A., Milli, S., Magri, D., 2015. Lateglacial – early Holocene vegetation history of the Tiber delta (Rome, Italy) under the influence of climate change and sea level rise. *Rev. Palaeobot. Palyno.* 218, 204–216.

Doglioni, C., 1993. Some remarks on the origin of foredeeps. *Tectonophysics* 228, 1–20.

Dormoy, I., Peyron, O., Combourieu Nebout, N., Goring, S., Kotthoff, U., Magny, M., Pross, J., 2009. Terrestrial climate variability and seasonality changes in the Mediterranean region between 15000 and 4000 years BP deduced from marine pollen records. *Clim. Past* 5, 615–632.

Fairbanks, R.G., 1989. A 17,000-year glacio-eustatic sea level record: influence of glacial melting rates on the Younger Dryas event and deep-ocean circulation. *Nature* 342, 637–642.

Favaretto, S., Asioli, A., Miola, A., Piva, A., 2009. Preboreal climatic oscillation recorded by pollen and foraminifera in the Southern Adriatic Sea. *Quat. Int.* 190, 89–102.

~~Ferrari, C. (editor), 1980. Flora e vegetazione dell'Emilia Romagna. Grafiche Zanini, Bologna (Italy), 1980.~~Ferrari, C. (editor), 1980. Flora e vegetazione dell'Emilia Romagna. Grafiche Zanini, Bologna (Italy), 1980.

Ferrari, C., 1997. The vegetation belts of Emilia Romagna (Northern Italy). *Allionia* 34, 219–231.

Feurdean, A., Wohlfarth, B., Björckman, L., Tantau, I., Bennike, O., Willis, K.J., Farcas, S., Robertsson, A.M., 2007. The influence of refugial populations on Lateglacial and early Holocene vegetational changes in Romania. *Rev. Palaeobot. Palyno.* 145, 305–320.

Fletcher, W.J., Zielhofer, C., 2011. Fragility of Western Mediterranean landscapes during Holocene rapid climate changes. *Catena* 103, 16–29.

Giraudi, C., Magny, M., Zanchetta, G., Drysdale, R.N., 2011. ~~The Holocene climatic evolution of Mediterranean Italy: a review of the continental geological data~~The Holocene climatic evolution of Mediterranean Italy: a review of the continental geological data. *The Holocene* 21 (1), 105–115.

Hammer, Ø., Harper, D.A.T., Ryan, P.D., 2001. PAST: Paleontological Statistics Software Package for Education and Data Analysis. *Palaeontol. Electron.* 4 (1). ~~9pp~~(9pp).

Jahns, S., van der Bogaard, C., 1998. New palynological and tephrostratigraphical investigations of two salt lagoons on the Island of Mljet, south Dalmatia, Croatia. *Veget. Hist. Archaeobot.* 7, 219–234.

Joannin, S., Vanni re, B., Galop, D., Peyron, O., Haas, J.N., Gilli, A., Chapron, E., Wirth, S.B., Anselmetti, F., Desmet, M., Magny, M., 2013. Climate and vegetation changes during the Lateglacial and early-middle Holocene at Lake Ledro (southern Alps, Italy). *Clim. Past* 9, 913–933.

Kaniewski, D., Van Campo, E., Paulissen, E., Weiss, H., Bakker, J., Rossignol, I., Van Lerberghe, K., 2011. ~~The Medieval climate anomaly and the Little Ice Age in coastal Syria inferred from pollen-derived palaeoclimatic patterns~~The medieval climate anomaly and the Little Ice Age in coastal Syria inferred from pollen-derived palaeoclimatic patterns. ~~Global Planet. Change~~Glob. Planet. Chang. 78, 178–187.

Lobo, F.J., Ridente, D., 2014. Stratigraphic architecture and spatio-temporal variability of high-frequency (Milankovitch) depositional cycles on modern continental margins: an overview. *Mar. Geol.* 352, 215–247.

Lowe, J.J., Accorsi, C.A., Bandini Mazzanti, M., Bishop, V., Van der Kaars, S., Forlani, L., Mercuri, A.M., Rivalenti, C., Torri, P., Watson, C., 1996. ~~Pollen stratigraphy of sediment sequences from carter lakes Albano and Nemi (near Rome) and from the central Adriatic, spanning the interval from oxygen isotope Stage 2 to the present day~~Pollen stratigraphy of sediment sequences from carter lakes Albano and Nemi (near Rome) and from the central Adriatic, spanning the interval from oxygen isotope stage 2 to the present day. *Mem. Ist. Ital. Idrobiol.* 55, 71–98.

Magny, M., de Beaulieu, J.-L., Drescher-Schneider, R., Vanni re, B., Walter-Simonnet, A.V., Miras, Y., Millet, L., Bossuet, G., Peyron, O., Brugiapaglia, E., Peyroux, A., 2007. ~~Holocene climate changes in the central Mediterranean as recorded by lake-level fluctuations at Lake Accesa (Tuscany, Italy)~~Holocene climate changes in the Central Mediterranean as recorded by Lake-level fluctuations at Lake Accesa (Tuscany, Italy). *Quat. Sci. Rev.* 26, 1736–1758.

Magny, M., Galop, D., Bellintani, P., Desmet, M., Didier, J., Haas, J.N., Martinelli, N., Pedrotti, A., Scandolari, R., Stock, A., Vanni re, B., 2009. Late Holocene climatic variability south of the Alps as recorded by lake-level fluctuations at Lake Ledro, Trentino, Italy. *The Holocene* 19 (4), 575–589.

Magny, M., Joannin, S., Galop, D., Vanni re, B., Haas, J.N., Bassetti, M., Bellintani, B., Scandolari, R., Desmet, M., 2012. Holocene palaeohydrological changes in the northern Mediterranean borderlands as reflected by the lake-level record of Lake Ledro, northeastern Italy. *Quat. Res.* 77, 382–396.

Magny, M., Combourieu-Nebout, N., de Beaulieu, J.L., Bout-Roumazielles, V., Colombaroli, D., Desprat, S., Francke, A., Joannin, S., Ortu, E., Peyron, O., Revel, M., Sadori, L., Siani, G., Sicre, M.A., Samartin, S., Simonneau, A., Tinner, W., Vanni re, B., Wagner, B., Zanchetta, G., Anselmetti, F., Brugiapaglia, E., Chapron, E., Debret, M., Desmet, M., Didier, J., Essallami, L., Galop, D., Gilli, A., Haas, J.N., Kallel, N., Millet, L., Stock, A., Turon, J.L., Wirth, S., 2013. North-South

- palaeohydrological contrasts in the central Mediterranean during the Holocene: tentative synthesis and working hypotheses. *Clim. Past* 9, 2043–2071.
- Mangerud, J., Andersen, S.T., Berglund, B.E., Dorrner, J.J., 1971. Quaternary stratigraphy of Norden, a proposal for terminology and classification. *Boreas* 3, 109–128.
- Maselli, V., Trincardi, F., 2013. Man made deltas. *Sci. Rep.* 2013 (3), 1926. doi:10.1038/srep01926.
- Mayewski, P.A., Rohling, E.E., Stager, J.C., Karlén, W., Maasch, K.A., Meecker, L.D., Meyerson, E.A., Gasse, F., van Kreveld, S., Holmgren, K., Lee-Thorp, J., Rosqvist, G., Rack, F., Staubwasser, M., Schneider, R.R., Steig, E.J., 2004. Holocene climate variability. *Quat. Res.* 62, 243–255.
- Mercuri, A.M., 2015. Applied palynology as a trans-discipline science: the contribution of aerobiology data to forensic and palaeoenvironmental issues. *Aerobiologia* 31, 323–339.
- Mercuri, A.M., Bandini Mazzanti, M., Torri, P., Vigliotti, L., Bosi, G., Florenzano, A., Olmi, L., Massamba N'siala, I., 2012. A marine/terrestrial integration for mid-late Holocene vegetation history and the development of the cultural landscape in the Po valley as a result of human impact and climate change. *Veget. Hist. Archeobot.* 21, 353–372.
- Peyron, O., Goring, S., Dormoy, I., Kotthoff, U., Pross, J., de Beaulieu, J.-L., Drescher Schneider, R., Vanni re, B., Magny, M., 2011. Holocene seasonality changes in the central Mediterranean region reconstructed from the pollen sequences of Lage Accessa (Italy) and Tenaghi Philippon (Greece). *The Holocene* 21 (1), 131–146.
- Peyron, O., Magny, M., Goring, S., Joannin, S., De Beaulieu, J.-L., Brugiapaglia, E., Sadori, L., Garfi, G., Kouli, K., Ioachim, C., Combourieu-Nebout, N., 2013. Contrasting patterns of climatic change during the Holocene across the Italian Peninsula reconstructed from pollen data. *Clim. Past* 9, 1233–1252.
- Pignatti, S., 1979. I piani di vegetazione in Italia. *Giorn. Bot. Ital.* 113, 411–428.
- Pignatti, S., 1982. *Flora d'Italia*. Edagricole, Bologna.
- Pignatti, S., 1998. *I boschi d'Italia – Sinecologia e biodiversit *. UTET, Torino.
- Pignatti, S., 2017. *Flora d'Italia*. Edagricole, Bologna.
- Pini, R., Minari, E., Furlanetto, G., Gorian, F., Ravazzi, C., Rizzi, A., Valoti, F., 2016. Guida per il riconoscimento del polline negli ambienti forestali della Pianura Padana. Tipografia Camuna S.p.A, Breno (Brescia, Italy).
- Piovan, S., Mozzi, P., Zecchin, M., 2012. The interplay between adjacent Adige and Po alluvial systems and deltas in the late Holocene (Northern Italy). *G omorphologie* 18 (4), 427–440.

Rasmussen, S.O., Vinther, B.M., Clausen, H.B., Andersen, V.V., 2007. Early Holocene climate oscillations recorded in three Greenland ice cores. *Quat. Sci. Rev.* 26, 1907–1914.

Rasmussen, S.O., Winther, B.M., Clausen, H.B., Andersen, K.K., 2007. ~~Early Holocene Greenland Ice Core Chronology 2005 (GICC05) and 10 year means of oxygen isotope data from ice core GRIP~~Early Holocene Greenland Ice Core Chronology 2005 (GICC05) and 10 Year Means of Oxygen Isotope Data from Ice Core GRIP. PANGAEA.

Rasmussen, S.O., Bigler, M., Blockley, S.P., Blunier, T., Buchardt, S.L., Clausen, H.B., Cvijanovic, I., Dahl-Jensen, D., Johnsen, S.J., Fischer, H., Gkinis, V., Guillevic, M., Hoek, W.Z., Lowe, J.J., Pedro, J.B., Popp, T., Seierstad, I.K., Steffensen, J.P., Svensson, A.M., Vallelonga, P., Vinther, B.M., Walker, M.J.C., Wheatley, J.J., Winstrup, M., 2014. ~~Dating, Synthesis, and Interpretation of Palaeoclimatic Records and Model-data Integration: Advances of the INTIMATE project~~Dating, Synthesis, and Interpretation of Palaeoclimatic Records and Model-data Integration: advances of the INTIMATE project. *Quat. Sci. Rev.* 106, 14–28.

Ravazzi, C. (Ed.), 2003. Gli antichi bacini lacustri e i fossili di Leffe, Ranica e Pianico-Sellere (Prealpi Lombarde). Quaderni di geodinamica alpina e quaternaria. CNR, Consiglio Nazionale delle Ricerche, Istituto per la dinamica dei processi ambientali.

Ravazzi, C., Marchetti, M., Zanon, M., Perego, R., Quirino, T., Deaddis, M., De Amicis, M., Margaritora, D., 2013. ~~Lake evolution and landscape history in the lower Mincio River valley, unravelling drainage changes in the central Po Plain (N-Italy) since the Bronze Age~~Lake evolution and landscape history in the lower Mincio River valley, unravelling drainage changes in the Central Po Plain (N-Italy) since the Bronze Age. *Quat. Int.* 288, 195–205.

Regione Emilia-Romagna & Eni-Agip, 1998. Riserve idriche sotterranee della Regione Emilia-Romagna. S.EL.CA, Firenze.

Regione Emilia-Romagna, Servizio Paesaggio, Parchi e Patrimonio Naturale, 1996. Cartografia fitoclimatica dell'Emilia Romagna. Carta 1:500.000. In: Assessorato Territorio, Programmazione e Ambiente, collana Studi e Documentazioni 47.

Reille, M., 1992. Pollen et spores d'Europe et d'Afrique du nord. Laboratoire de Botanique Historique et Palynologie, Marseille.

Reille, M., 1995. Pollen et spores d'Europe et d'Afrique du nord. Supplément 1. Laboratoire de Botanique Historique et Palynologie, Marseille.

Reille, M., 1998. Pollen et spores d'Europe et d'Afrique du nord. Supplément 2. Laboratoire de Botanique Historique et Palynologie, Marseille.

Reimer, P.J., Bard, E., Bayliss, A., Warren Beck, J., Blackwell, P.G., Bronk Ramsey, C., Buck, C.E., Cheng, H., Lawrence Edwards, R., Friedrich, M., Grootes, P.M., Guilderson, T.P., Haflidason, H., Hajdas, I., Hatté, C., Heaton, T.J., Hoffmann, D.L., Hogg, A.G., Hughen, K.A., Felix Kaiser, K.,

Kromer, B., Manning, S.W., Niu, M., Reimer, R.W., Richards, D.A., Marian Scott, E., Southon, J.R., Staff, R.A., Turney, C.S.M., Van der Plicht, J., 2013. Intcal13 and Marine13 radiocarbon age calibration curves 0-50,000 years cal BP. *Radiocarbon* 55, 1869–1887.

Ricci Lucchi, F., Colalongo, M.L., Cremonini, G., Gasperi, G., Iaccarino, S., Papani, G., Raffi, S., Rio, D., 1982. Evoluzione sedimentaria e paleogeografica nel margine appenninico. In: Cremonini, G., Ricci Lucchi, F. (Eds.), *Guida alla geologia del margine Appenninico–Padano*. Guida Geologica Regionale della Società Geologica Italiana. pp. 17–46.

Roberts, N., Allcock, S.L., Barnett, H., Mather, A., Eastwood, W.J., Jones, M., Primmer, N., Yiğitbaşıoğlu, H., Vannière, B., 2019. ~~Cause-and-effect in Mediterranean erosion: The role of humans and climate upon Holocene sediment flux into a central Anatolian lake catchment~~Cause-and-effect in Mediterranean erosion: the role of humans and climate upon Holocene sediment flux into a central Anatolian lake catchment. *Geomorphology* 331, 36–48.

Rossi, V., Vaiani, S.C., 2008. Microfaunal response to sediment supply changes and fluvial drainage reorganization in Holocene deposits of the Po Delta, Italy. ~~Mar. Micropaleontol.~~Mar. Micropaleontol. 69, 106–118.

Sadori, L., Jahns, S., Peyron, O., 2011. Mid-Holocene vegetation history of the central Mediterranean. *The Holocene* 21 (1), 117–129.

Sangiorgi, F., Capotondi, L., Combourieu-Nebout, N., Vigliotti, L., Brinkhuis, H., Giunta, S., Lotter, A.F., Morigi, C., Negri, A., Reichert, G.-J., 2003. Holocene seasonal sea-surface temperature variations in the southern Adriatic Sea inferred from a multiproxy approach. *J. Quat. Sci.* 18 (8), 723–732.

Sarti, G., Rossi, V., Amorosi, A., Bini, M., Giacomelli, S., Pappalardo, M., Ribecai, C., Ribollini, A., Sammartino, I., 2015. Climatic signature of two mid-late Holocene fluvial incisions formed under sea-level highstand conditions (Pisa coastal plain, NW Tuscany, Italy). ~~Palaeogeogr.–Palaeoclimatol.–Palaeoecol.~~Palaeogeogr. Palaeoclimatol. Palaeoecol. 434, 183–195.

Scarponi, D., Azzarone, M., Kowalewski, M., Huntley, J.W., 2017. Surges in trematode prevalence linked to centennial-scale flooding events in the Adriatic. *Sci. Rep.* 7, 5732. doi:10.1038/s41598-017-05979-6.

Signell, R.P., Chiggiato, J., Horstmann, J., Doyle, J.D., Pullen, J., Askari, F., 2010. High resolution mapping of Bora winds in the northern Adriatic Sea using synthetic aperture radar. *J. Geophys. Res.* 115, C04020.

Stefani, M., Vincenzi, S., 2005. The interplay of eustasy, climate and human activity in the late Quaternary depositional evolution and sedimentary architecture of the Po Delta system. *Mar. Geol.* 222–223, 19–48.

Styllas, M.N., Ghilardi, M., 2017. ~~Early- to mid-Holocene paleohydrology in northeast Mediterranean: The detrital record of Aliakmon River in Loudias Lake, Greece~~Early- to mid-Holocene paleohydrology

[in northeast Mediterranean: the detrital record of Aliakmon River in Loudias Lake, Greece](#). *The Holocene* 27, 1487–1498.

Subally, D., Quézel, P., 2002. Glacial or interglacial: *Artemisia*, a plant indicator with dual responses. *Rev. Palaeobot. Palyno.* 120, 123–130.

Tarasov, P.E., Cheddadi, R., Guiot, J., Bottema, S., Peyron, O., Belmonte, J., Ruiz-Sanchez, V., Saadi, F., Brewer, S., 1998. A method to determine warm and cool steppe biomes from pollen data; application to the Mediterranean and Kazakhstan regions. *J. Quat. Sci.* 13 (4), 335–344.

Tomaselli, M., 1970. Note illustrative alla carta della vegetazione naturale potenziale d'Italia. Min. Agr. Foreste, Collana verde 27, Roma.

Tomaselli, M. (Ed.), 1987. Guida alla vegetazione dell'Emilia Romagna. Collana Annali, Facoltà di Scienze MM., FF., NN. Università di Parma.

Tutin, T.G., Heywood, V.H., Burges, N.A., Valentine, D.H., 1993. *Flora europaea*. Cambridge University Press.

Tüxen, R., 1956. Die heutige potentielle natürliche Vegetation als Gegenstand der Vegetationskartierung. *Angewandte Pflanzensoziologie (Stolzenau)* 13, 4–42.

Ubaldi, D., 2003. Flora, fitocenosi e ambiente. In: *Elementi di geobotanica e fitosociologia*. CLUEB, Bologna.

Vacchi, M., Marriner, N., Morhange, C., Spada, G., Fontana, A., Rovere, A., 2016. Multiproxy assessment of Holocene relative sea-level changes in the western Mediterranean: sea-level variability and improvements in the definition of the isostatic signal. *Earth-Sci. Rev.* 155, 172–197.

Valsecchi, V., Finsinger, W., Tinner, W., Ammann, B., 2011. Testing the influence of climate, human impact and fire on the Holocene population expansion of *Fagus sylvatica* in the southern Prealps (Italy). *The Holocene* 18 (4), 603–614.

Vannièrè, B., Power, M.J., Roberts, N., Tinner, W., Carriòn, J., Magny, M., Bartlein, P., Colombaroli, D., Daniau, A.L., Finsinger, W., Gil-Romera, G., Kaltenrieder, P., Pini, R., Sadori, L., Turner, R., Valsecchi, V., Vescovi, E., 2011. Circum-mediterranean fire activity and climate changes during the mid-Holocene environmental transition (8500-2500 cal. BP). *The Holocene* 21 (1), 53–73.

Vescovi, E., Kaltenrieder, P., Tinner, W., 2018. Late-Glacial and Holocene vegetation history of Pavullo nel Frignano (Northern Apennines, Italy). *Rev. Palaeobot. Palyno.* 160, 32–45.

Walker, M., Berkelhammer, M., Björck, S., Cwynar, L., Fisher, D.A., Long, A.J., Lowe, J.J., Newnham, R.M., Rasmussen, S.O., Weiss, H., 2012. Formal subdivision of the Holocene Series/Epoch: a discussion paper by working group of INTIMATE (Integration of ice-core, marine and terrestrial records) and the Subcommittee on Quaternary Stratigraphy (International Commission of Stratigraphy). *J. Quat. Sci.* 27 (7), 649–659.



Walker, M., Head, M.J., Berkelhammer, M., Björck, S., Cheng, H., Cwynar, L., Fisher, D., Gkinis, V., Long, L., Lowe, J., Newnham, R., Rasmussen, S.O., Weiss, H., 2018. Formal ratification of the subdivision of the Holocene Series/ Epoch (Quaternary System/Period): two new Global Boundary Stratotype Sections and Points (GSSPs) and three new stages/ subseries. *Episodes* 41 (4), 213–223. doi:10.18814/epiiugs/2018/018016.

Watts, W.A., Allen, J.R.M., Huntley, B., 1996. ~~Vegetation history and palaeoclimate of the Last Glacial period at Lago Grande di Monticchio, Southern Italy~~ Vegetation history and palaeoclimate of the last Glacial period at Lago Grande di Monticchio, Southern Italy. *Quat. Sci. Rev.* 15, 133–153.

Zhornyak, L.V., Zanchetta, G., Drysdale, R.N., Hellstrom, J.C., Isola, I., Regattieri, E., Piccini, L., Baneschi, I., Couchoud, I., 2011. Stratigraphic evidence for a “pluvial phase” between ca 8200-7100 ka from Renella cave (Central Italy). *Quat. Sci. Rev.* 30, 409–417.

---

## Highlights

- Coastal plains are useful depositional archive for palaeoclimate investigations.
- A palyno-stratigraphic approach can distinguish environmental from climate changes.
- The Holocene vegetation-climate variability fits with a series of Bond events.
- The 8.2 ka cooling event has an evident vegetation and stratigraphic expression.
- Holocene climate changes affect coastal sedimentation and fluvial activity.

---

Thirty-five samples from the uppermost 25 metres were collected for palynological analysis. All lithofacies were analysed with a special focus on organic-rich intervals, where abundant palynological assemblages were expected. Samples were prepared and analysed at “*Centro Agricoltura e Ambiente – CAA G. Nicoli*” laboratory (Italy), following a standard extraction technique (Lowe et al., 1996): about 3–9 g of dry sediment were weighed and a *Lycopodium* tablet was added to calculate pollen concentration. Samples were mechanically disrupted in a 10% Na-pyrophosphate solution and filtered through a 0.5 mm sieve and a 5 µm nylon filter. A series of chemical treatments was then applied (10% HCl solution to remove carbonates, acetolysis for excess organics, heavy liquid, 40% HF solution, ethanol suspension for pollen grains enrichment). Following evaporation at 60 °C, microscope slides were prepared with glycerine jelly and paraffin. For each sample, at least 300 pollen grains were counted (where possible) at 400~~x~~ magnification and recognised using general morphological keys (Faegri et al., 1989; Moore et al., 1991). The CAA laboratory’s collection and published atlases (Reille, 1992, 1995, 1998) were also useful to improve pollen determination. If the conservation degree and orientation (i.e., polar or equatorial view) of grains were favourable, a set of morphological parameters published in literature were used for the determination at species level of alders, oaks, pines and Asteroideae (*SOM-SI*). If this was not possible, the conservative choice of the higher taxonomical level was made to avoid mis/overinterpretation.

The following are the supplementary data related to this article.

[Multimedia Component 1](#)

~~SOM-S1~~:[SOM-S1](#)

Summary of the pollen keys and references used for taxonomic identification of alders, oaks, pines and Asteroideae.

alt-text: SOM-S1

[Multimedia Component 2](#)

~~SOM - Table S1~~:[SOM - Table S1](#)

Raw counts of the 189 identified taxa.

alt-text: SOM - Table S1

## Queries and Answers

**Query:** Your article is registered as a regular item and is being processed for inclusion in a regular issue of the journal. If this is NOT correct and your article belongs to a Special Issue/Collection please contact [s.sankaran@elsevier.com](mailto:s.sankaran@elsevier.com) immediately prior to returning your corrections.

**Answer:**

**Query:** Please confirm that given names and surnames have been identified correctly and are presented in the desired order, and please carefully verify the spelling of all authors' names.

**Answer:**

**Query:** The author names have been tagged as given names and surnames (surnames are highlighted in teal color). Please confirm if they have been identified correctly.

**Answer:**

**Query:** Please check the hierarchy of the section headings and confirm if correct.

**Answer:**

**Query:** Citation "Bond et al., 1993" has not been found in the reference list. Please supply full details for this reference.

**Answer:**

**Query:** The citation “Walker et al., 2009” has been changed to “Walker et al., 2012” to match the author name/date in the reference list. Please check if the change is fine in this occurrence and modify the subsequent occurrences, if necessary.

**Answer:**

**Query:** Citation "International Commission on Stratigraphy, 2018" has not been found in the reference list. Please supply full details for this reference.

**Answer:**

**Query:** The citation “Feurdean et al., 2014” has been changed to “Feurdean et al., 2007” to match the author name/date in the reference list. Please check if the change is fine in this occurrence and modify the subsequent occurrences, if necessary.

**Answer:**

**Query:** Citation "Faegri et al., 1989" has not been found in the reference list. Please supply full details for this reference.

**Answer:**

**Query:** Citation "Moore et al., 1991" has not been found in the reference list. Please supply full details for this reference.

**Answer:**

**Query:** The citation “Bondesan et al., 1995” has been changed to “Bondesan et al., 1999” to match the author name/date in the reference list. Please check if the change is fine in this occurrence and modify the subsequent occurrences, if necessary.

**Answer:**

**Query:** Citation "Chiarucci et al., 2010" has not been found in the reference list. Please supply full details for this reference.

**Answer:**

**Query:** Citation "Hengl et al., 2018" has not been found in the reference list. Please supply full details for this reference.

**Answer:**

**Query:** Citation "Ferrari et al., 1997" has not been found in the reference list. Please supply full details for this reference.

**Answer:**

**Query:** The citation "Valsecchi et al., 2008" has been changed to "Valsecchi et al., 2011" to match the author name/date in the reference list. Please check if the change is fine in this occurrence and modify the subsequent occurrences, if necessary.

**Answer:**

**Query:** The citation "Rasmussen et al., 2007" has been changed to "Rasmussen et al., 2007a, b" to match the author name/date in the reference list. Please check if the change is fine in this occurrence and modify the subsequent occurrences, if necessary.

**Answer:**

**Query:** The citation "Mercuri et al., 2015" has been changed to "Mercuri, 2015" to match the author name/date in the reference list. Please check if the change is fine in this occurrence and modify the subsequent occurrences, if necessary.

**Answer:**

**Query:** Citation "Fletcher and Zielhofer (2013)" has not been found in the reference list. Please supply full details for this reference.

**Answer:**

**Query:** The citation "Mangerud et al. (1974)" has been changed to "Mangerud et al. (1971)" to match the author name/date in the reference list. Please check if the change is fine in this occurrence and modify the subsequent occurrences, if necessary.

**Answer:**

**Query:** The citation "Amorosi et al., 2017" has been changed to "Amorosi et al., 2017a, b" to match the author name/date in the reference list. Please check if the change is fine in this occurrence and modify the subsequent occurrences, if necessary.

**Answer:**

**Query:** Uncited references: This section comprises references that occur in the reference list but not in the body of the text. Please position each reference in the text or, alternatively, delete it. Thank you.

**Answer:**

**Query:** Have we correctly interpreted the following funding source(s) and country names you cited in your article:

"Marco Polo Programme".

**Answer:**